JOURNAL OF GEOPHYSICAL RESEARCH, VOL. 106, NO. C6, PAGES 11,505–11,527, JUNE 15, 2001

Wind and Gulf Stream influences on along-shelf transport and off-shelf export at Cape Hatteras, North Carolina

Dana K. Savidge[1] and John M. Bane Jr.

Department of Marine Sciences, University of North Carolina at Chapel Hill, Chapel Hill, North Carolina.

Abstract. Along-shelf transports across three cross-shelf lines on the continental shelf near Cape Hatteras have been calculated from moored current meter data over a continuous 24 month period in 1992-1994. The along-shelf convergence has been used to infer off-shelf export. Transport and transport convergence have been related to wind and Gulf Stream forcing and to variability in sea level at the coast. The along-shelf transport variability is primarily wind-driven and highly correlated with sea level fluctuations at the coast. Both winds and along-shelf transport exhibit a near-annual period variability. Along-shelf transport is not well correlated with Gulf Stream offshore position. Along-shelf transport convergence is highly correlated with Gulf Stream position offshore, with a more shoreward Gulf Stream position leading increased along-shelf convergence by hours to a few days. Long-period variability of 14-16 months and 1-3 months is apparent in both Gulf Stream position and transport convergence. Variability in along-shelf convergence is poorly correlated with wind, wind convergence, or coastal sea level. A likely hypothesis accounting for the observed relationship between Gulf Stream position and along-shelf transport convergence is that the Gulf Stream is directly influencing cross-shelf export processes along the outer boundary of the study site. Despite predominantly convergent flow on the shelf at Cape Hatteras, brief periods of along-shelf divergence and shoreward cross-shelf transport exist ($\sim$10% of the time just north of Cape Hatteras and $\sim$34% of the time just south of Cape Hatteras during episodes of up to 3-8 days duration). Implied onshore flows of a few cm s^{-1} are tentatively identified in the moored current meter data for these periods. Satellite imagery for an extended along-shelf divergent period clearly suggests that shelf edge parcels could be advected a significant fraction of the way across the shelf.

1. Introduction and Background

The coastal ocean in the vicinity of Cape Hatteras, North Carolina, is characterized by a complex flow regime. Wind forcing, changes in coastline orientation, variable bathymetry, and along-shelf and cross-shelf horizontal pressure gradients caused by both sea surface slopes and horizontal density gradients contribute to that complexity. Here Mid-Atlantic Bight (MAB) and South Atlantic Bight (SAB) shelf waters meet, and a large freshwater influx enters the coastal ocean from the landward edge [*Manning*, 1991]. Gulf Stream meanders progress past the cape [*Glenn and Ebbesmeyer*, 1994a], possibly decaying and importing slope water into the coastal regime [*Lee et al.*, 1991]. Gulf Stream filaments overwash the narrow shelf and participate in various mechanisms of shelf water export to the open ocean [*Lillibridge et al.*,1990;*Churchill and Cornillon*,1991;*Glenn and Ebbesmeyer*,1994a ;*Churchill and Berger*, 1998].

One integrated way to address the net effect of these processes is through the assessment of volume transport. Volume transport on the continental shelf near Cape Hatteras is of interest for a variety of reasons, spanning essentially all subdisciplines within coastal oceanography. In recent years, proposed gas and oil drilling sites on the shelf and slope have made the oceanographic regime there of particular interest to geologists, ecologists, and environmental scientists. It is a region of biological significance, as many fish and other fauna utilize the adjacent Albemarle and Pamlico Sounds and the nearby Cheasapeake Bay as nursury grounds. Some of these species spawn on the midshelf to outer shelf, far removed from the coastal and estuarine regimes into which their larvae must migrate [*Checkley et al.*, 1988; *Hare and Cowen*, 1991, 1996; *Stegmann and Yoder*, 1996; *Quinlan et al.*, 1999]. It is also a region where interest has focused on the flux (or lack thereof) of particulate organic matter to the open ocean [*Walsh et al.*, 1988; *Biscaye et al.*, 1994].

In this paper, along-shelf volume transports across three cross-shelf lines on the continental shelf near Cape Hatteras

[1]Now at Center for Coastal Physical Oceanography, Department of Ocean, Earth and Atmospheric Sciences, Old Dominion University, Norfolk, Virginia.

Paper number 2000JC000574.
0148-0227/01/2000JC000574$09.00

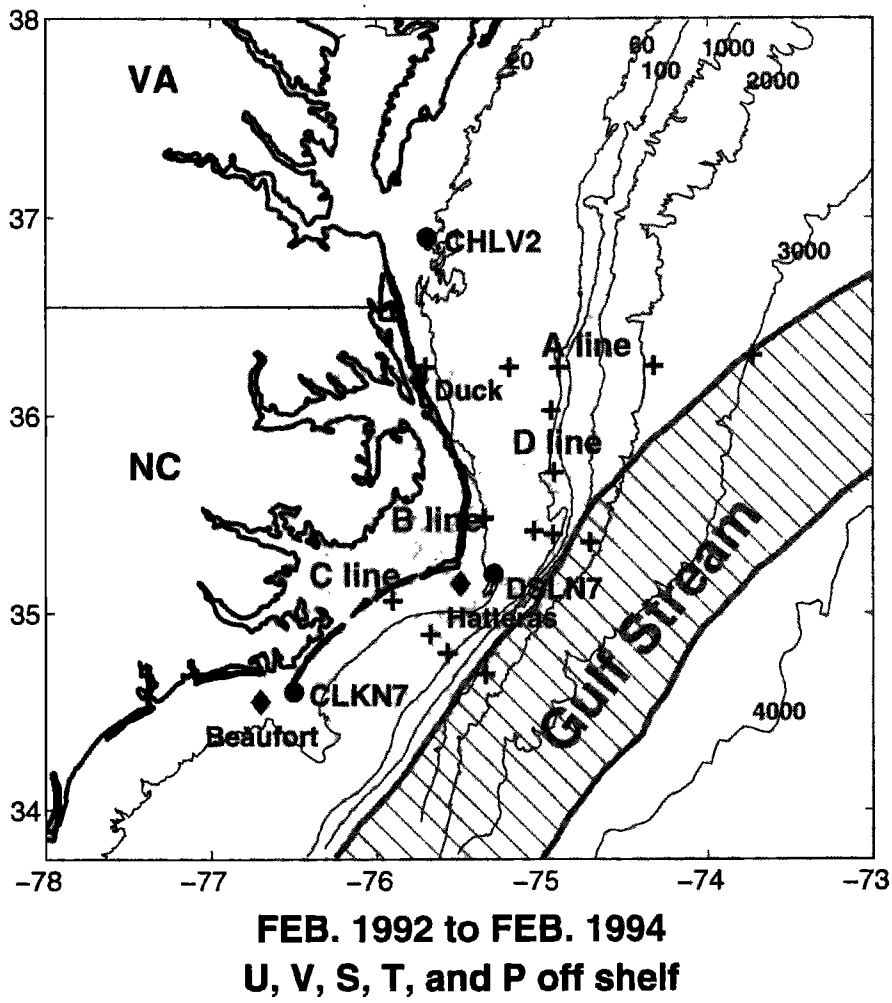

Figure 1. Cape Hatteras continental shelf/slope field study site. Fifteen mooring locations across and along the Cape Hatteras shelf and slope were maintained from March 1992 through February 1994. These moorings were situated along three cross-shelf lines, designated from north to south as lines A, B, and C, and along one shelf edge line oriented north-south, designated line D. Mooring numbers increment from 1 to 4 or 5 in the offshore direction. Line D moorings increment north to south. Mooring locations (pluses), Coastal Marine Automated Network (C-MAN) meteorological stations (solid circles), and sea level stations (solid diamonds) are shown. A schematic Gulf Stream is shown, which approximately follows the 200 m isobath south of Cape Hatteras, then separates from the continental shelf north of Cape Hatteras.

are calculated from moored current meter data over a continuous 24 month period. The along-shelf transport convergence has been calculated and has been used to infer cross-shelf transport, assuming continuity and no flow through the shoreward boundary. Transport and transport convergence have been related to wind and Gulf Stream forcing and to variability in sea level at the coast.

The data used in this study were collected by a multi-institutional team funded by the Minerals Management Service [*Berger et al.*, 1995]. Fifteen mooring locations across and along the Cape Hatteras shelf and slope were maintained from March 1992 through February 1994 (Figures 1 and 2). These moorings were situated along three cross-shelf lines, designated from north to south as lines A, B, and C, and along one shelf edge line oriented north-south, designated line D. Full details of the deployments and data processing are available in a series of data reports prepared during and after the project [*Berger et al.*, 1995]. Other components of the project included periodic hydrographic sections, drifter releases, and collection of satellite sea surface temperature imagery. Preliminary findings were summarized in a technical report at the conclusion of the project [*Berger et al.*, 1995]. Findings most relevant to the present work are as follows. Principal axes of flow variance on the shelf were primarily along-shelf, with along-shelf convergence in the mean near Cape Hatteras (Figure 3). Flow on the shelf was highly coherent, both from site to site and with depth. The outermost slope moorings on each line were imbedded in the Gulf Stream flow for most of the project duration, showing strong, coherent, primarily northeastward flow at 100 and 300 m depths. In addition, flow at the shelf edge (along the 60 m isobath) on lines B and C was often quite coherent with

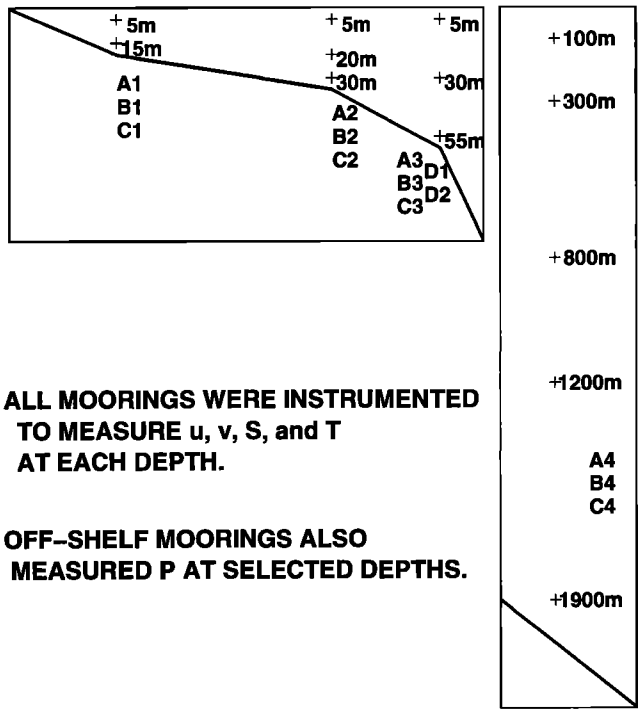

Figure 2. Schematic mooring line design. Shelf moorings were situated at the 20, 35, and 60 m isobaths, with slope moorings at the 2000 m isobath. The A line had an additional mooring at the 3000 m isobath. Shelf edge mooring line D was situated between lines A and B along the 60 m isobath. Subscripts indicate instrument packages on a single line, incrementing top to bottom. For example, the 300 m depth package on the mooring in 2000 m depth water on the northernmost line is refered to as $A4_2$. (left) Shelf and shelf edge moorings had 2-3 instrument packages in the vertical, including InterOcean S4 and General Oceanic MkII winged current meters, temperature and salinity sensors. (right) Deeper moorings had 5-6 instrument packages in the vertical, including General Oceanic MkI/MkII winged current meters and Aanderaa RCM 7/8s, temperature, salinity, and pressure sensors. Right panel: slope moorings had 5-6 instrument packages in the vertical, including General Oceanic MkI/MkII winged current meters and Aanderaa RCM 7/8s, temperature, salinity, and pressure sensors. Moorings A4, B4, and C4 were instrumented as shown. Mooring A5 had an additional package at 2900 m.

the Gulf Stream flow at the outermost moorings, with speeds occasionally in excess of 1 m s^{-1}. In contrast, shelf edge velocities on lines A and D were only occasionally strongly northeastward and so did not appear to be characteristic of the Gulf Stream jet. In summer, midshelf (at the 35 m isobath) velocities on lines B and C also showed occasional coherence with those at the outermost moorings. An offshore increase in current magnitude is evident between the 35 and 60 m isobaths along all three mooring lines. Mean flow measured between the shelf edge mooring and the outermost slope mooring on line A was southeastward at 100 and 300 m depths and was apparently imbedded in the Slope Sea Gyre circulation.

Berger et al. [1995] found evidence for a variety of mechanisms forcing the flow on the shelf and slope in this region. Coherence in along-shelf velocity across the shelf shows a peak at 5-8 days, at 16-20 days, and on longer timescales, especially at 50-60 days. The shelf flow was strongly coherent with the wind at the weekly timescale. The weekly timescale is also characteristic of Gulf Stream meander propagation past Cape Hatteras, and the energetic Gulf Stream can affect flow over the entire shelf in a variety of ways. The coherence of the outer-shelf moorings with the Gulf Stream-imbedded moorings is evidence of direct Gulf Stream forcing and/or flow on the shelf. The cross-shelf increase in current magnitude is also likely a Gulf Stream effect, either through entrainment or cross-shelf sea surface slope effects. Gulf Stream filaments often overwash the entire shelf just south of Cape Hatteras [*Glenn and Ebbesmeyer*, 1994b]. Gulf Stream offshore location, separation angle, and path curvature at the Cape affect filament size and production, coastal sea level, and cross-shelf sea level slope. Changes in these Gulf Stream factors can advect existing temperature and salinity fronts across the shelf. *Churchill and Berger* [1998] found the advection along moving density fronts to be an important factor contributing to offshore export of shelf water here. One important front that extends across the shelf, typically diagonally from the northeast to the southwest, separates MAB shelf water from SAB shelf water. Freshwater export from the Chesapeake Bay and the North Carolina sounds contributes to the existence of density driven flows. Finally, along-shelf pressure gradients have been postulated to exist both in the SAB and the MAB [*Csanady*, 1979; *Lee et al.*, 1985]. These pressure gradient forces are directed toward the Cape and presumably

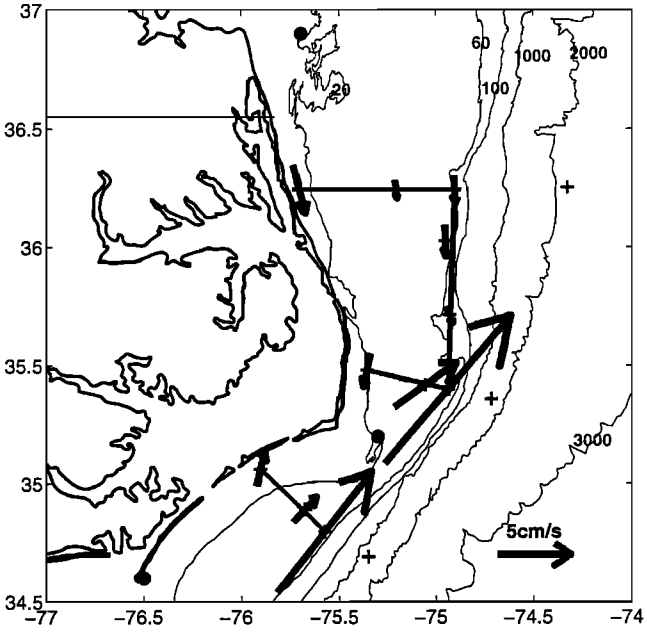

Figure 3. Average velocity at shelf mooring locations. Values are weighted averages from all instrument depths on each mooring. Mooring locations (pluses) and C-MAN meteorological stations (solid circles) are shown.

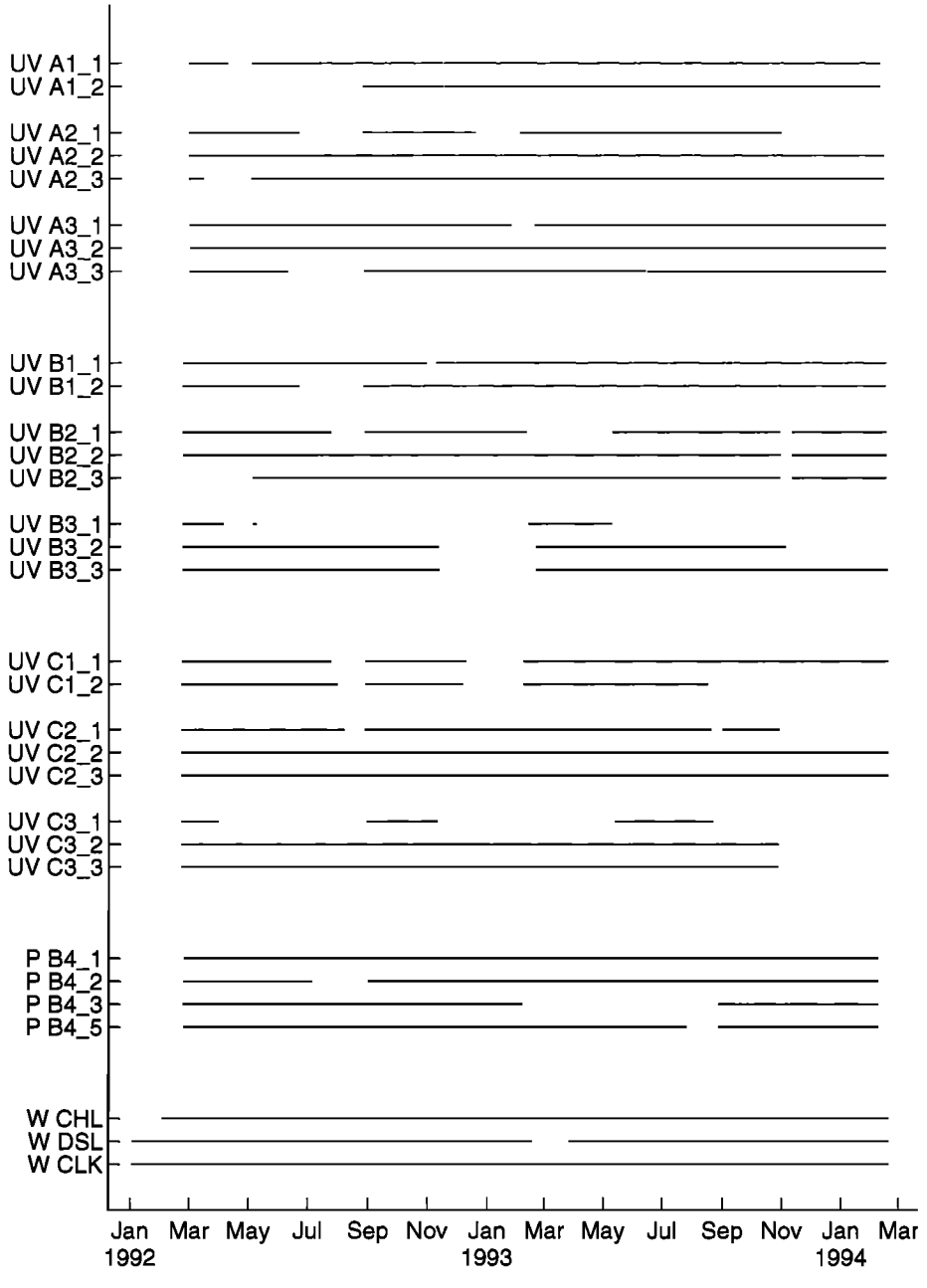

Figure 4. Shelf mooring velocity, P_{B4_1}, and C-MAN wind station data return time lines. Instrument packages on particular moorings are numbered sequentially downward. For example, the 55 m package at B3 is designated $B3_3$. Missing data are represented by gaps in the lines.

contribute to mean flows along-shelf toward Cape Hatteras in both the SAB and the MAB.

2. Key Variables

2.1. Winds

Wind data from three Coastal Marine Automated Network (C-MAN) stations located near Cape Hatteras were used in this study (Figure 1): CHLV2, near Cape Henry on the southern side of Cheasapeake Bay; DSLN7, off Cape Hatteras over Diamond Shoals; and CLKN7, off Cape Lookout. These data were 48 hour low-passed using a Hanning filter and subsampled at 1 day intervals. Variability in the wind was highly coherent along the shelf. In the following the CHLV2 and DSLN7 records are both used to represent shelf winds for the experiment period. Short gaps in the DSLN7 data were filled with CLKN7 winds, with means and standard deviations adjusted to match those at DSLN7 (see Figure 4). Calculations of along-shelf divergence in the winds were made by rotating the winds into along- and across-shelf components and taking the difference between the CHLV2 and DSLN7 along-shelf records. The along-shelf directions for CHLV2 and DSLN7 were assumed to be the direction of the principal axis of variability for moorings $A2_2$ and $B2_2$ (the midshelf, mid-water column mooring from the nearest mooring lines), respectively. The rotations were -17° and

17° clockwise from true north, respectively. Primary results discussed below are equivalent if along-shelf is defined as true north for each location.

2.2. Gulf Stream Position

Some measure of Gulf Stream variability is necessary to explore its effect on shelf transport. One commonly used variable is distance from the shore or shelf edge to the shoreward edge of the stream. This is relevant because of the effect this distance has on how Gulf Stream frontal eddies and filaments form and proceed downstream, how water is upwelled shoreward of the stream, how the strong Gulf Stream currents impinge on the shallow shelf regions, and how the sea surface topography associated with the stream affects sea surface slope on the shelf. Typically, the distance from shore or shelf edge to the stream is measured by inspecting advanced very high resolution radiometer (AVHRR) sea surface temperature (SST) imagery for the main Gulf Stream temperature front along some transect oriented perpendicular to the coastline. For the present work, a sensible transect to choose would be mooring line B since it is central to the mooring lines discussed here and is at the southern edge of the northernmost box defined by mooring lines A, B, and C, where most of the following work focuses. However, this proved to be a particularly difficult region in which to reliably determine Gulf Stream location to the accuracy required over a continuous 2 year time span. The Gulf Stream meander envelope is particularly narrow at this location, the Cape Hatteras cross-shelf front meets the Gulf Stream front in this immediate vicinity, and the narrow shelf here is often overwashed with warm water of presumably Gulf Stream origin. In fact, a front of some sort is almost always present right over mooring B3. Efforts to manually select the Gulf Stream front from satellite imagery proved insufficient. Instead, a new method of determining the offshore position of the Gulf Stream was developed.

As discussed in section 1, mooring B4 was imbedded in the Gulf Stream's cyclonic flank throughout most of the experiment. (See Figure 2 for elaboration of the instrument packages and mooring naming conventions.) Of the variables measured by the uppermost instrument package there, horizontal current direction (α) and magnitude (V), converted to eastward and northward components (u and v), temperature (T), salinity (S), and pressure (P), P proves to be most useful as an indicator of Gulf Stream position. If the mooring line were rigid, each current meter and T sensor would stay at the same depth in the water throughout the measurement period. In that case both T and V would in-

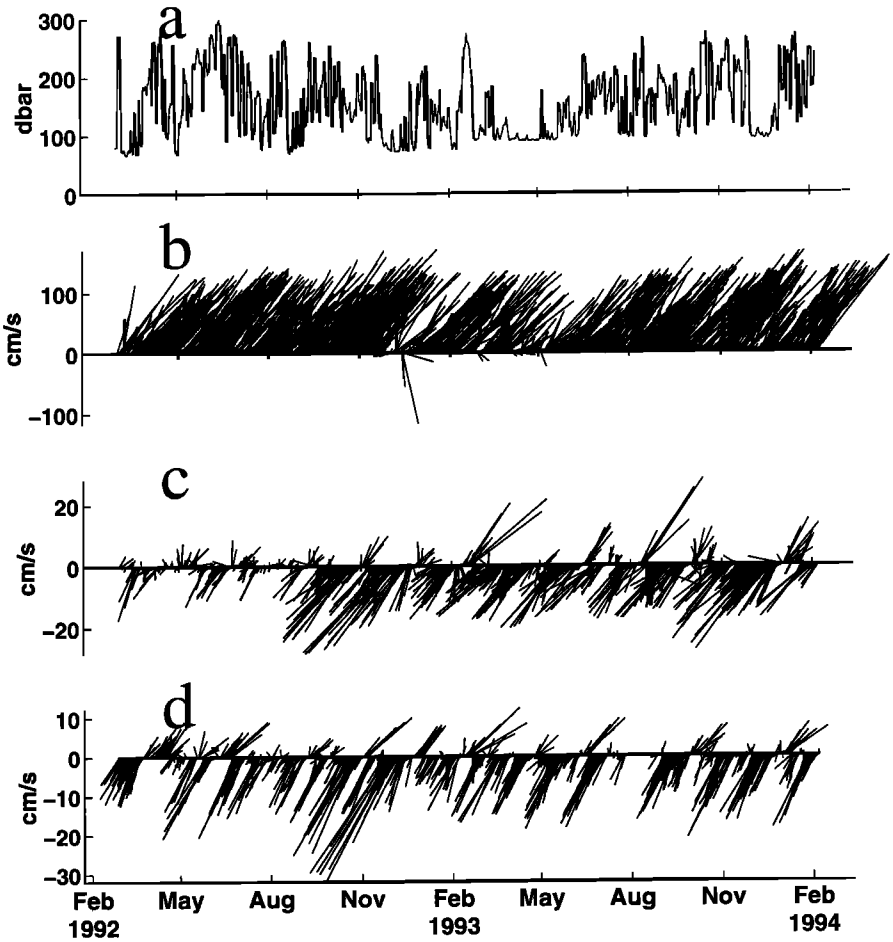

Figure 5. Selected daily 48 hour low-passed time series from mooring B_4: (a) the pressure record at 100 m (target) depth and velocity sticks at (b) 100, (c) 1200, and (d) 1900 m depths. Sticks oriented vertically represent northward velocity.

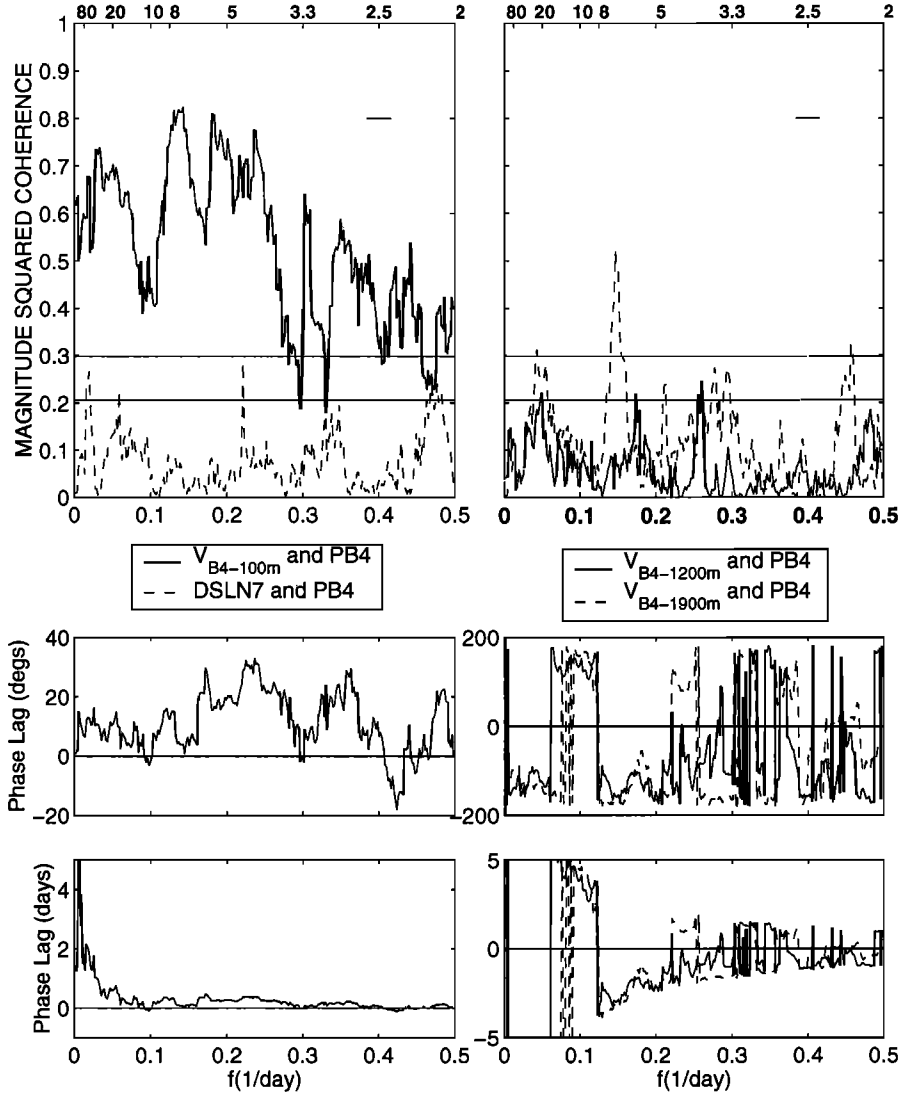

Figure 6. Cross spectra between selected time series at mooring B_4: (left) cross spectra between DSLN7 along-shelf wind and P_{B4_1} and between 100 m depth velocity magnitudes and P_{B4_1}, (right) cross spectra between 1200 m depth velocity magnitudes and P_{B4_1} and between 1900 m depth velocity magnitudes and P_{B4_1}, (top) magnitude squared coherence (drawn to the same scale), (middle) the phase lag in degrees, and (bottom) the phase lag in days, converted from degrees by $\theta_{day} = \theta_{deg}/(f360)$, where f is frequency. Positive phase lags indicate that the first quantity in the pair leads the second. Horizontal lines in the top panels show the 99% and 95% confidence levels.

crease as the cyclonic flank of the Gulf Stream moved closer to the shelf edge. However, since the mooring is not rigid, as the Gulf Stream jet shifts toward the shelf edge, the mooring line is pulled down in the water column by the integrated effect of the large Gulf Stream currents [*Hogg*, 1991]. Since T and V fall off with depth in the cyclonic side of the Gulf Stream, this effect will compete with the expected increase in T and V as the Gulf Stream axis nears the shelf and tilts the mooring. This confounds the usefulness of either T or V at a given mooring as an indicator of where in the stream the mooring is. The cross-stream S structure of the Gulf Stream is less well characterized than the fairly robust and well-known T or V cross-sections, and the S measurements from these mooring packages would suffer from the same difficulty as the T or V records: decreasing S with depth would confound the usefulness of increasing S seaward across the Gulf Stream as an indicator of cross-stream position. However, the pressure records indicate how far in the vertical the particular mooring has been dragged down and varies monotonically with the depth-integrated V impinging on the mooring line. In the vicinity of mooring B4 several types of energetic currents may be impinging on the mooring line. The Gulf Stream edge occupies the upper 300 m or more of the water column. *Berger et al.* [1995] found that the 100 and 300 m depth meters were highly correlated and exhibited strong northeastward means, while at 800 m and below the flow was coherent but weak and uncorrelated with the surface flow. Gulf Stream filaments periodically exhibit or-

ganized and energetic flow over the upper 100 m or more of the upper water column. The Deep Western Boundary Current crosses under the Gulf Stream, and though it exhibits much smaller maximum velocities than the Gulf Stream, its influence is spread over much of the subthermocline water column [*Pickart and Smethie*, 1994]. Finally, topographic Rossby waves are known to traverse the region in the subthermocline ocean [*Johns and Watts*, 1986]. These velocities can exceed 0.20 m s^{-1} and extend over much of the subthermocline ocean as well. Visual inspection of velocity records at 100, 1200, and 1900 m depth at mooring B4 indicate that the Gulf Stream motion appears to dominate the B4 100 m pressure records (P_{B4_1}) (Figure 5) as the pressure fluctuations are strongly correlated with episodes of strong northeastward flow in the upper current meter records and not with strong southwestward filament pulses in the upper water column nor with lower water column fluctuations. Cross spectra indicate high correlation between P_{B4_1} and the B4 100 m velocity magnitudes ($VB4_1$) across a wide range of frequencies, but low correlation between P_{B4_1} and the B4 1200 m velocity magnitudes (V_{B4_4}) or the B4 1900 m velocity magnitudes (V_{B4_5}) (Figure 6). An interesting exception is the high coherence between V_{B4_5} and P_{B4_1} at the 7.5 day period. These are presumably topographic Rossby waves [*Berger et al.*, 1995]. The upper level velocities typically lead pressure fluctuations by 0.25-0.5 days over the 2-10 day band, increasing to leads of a few days for the longest resolved periods.

It seems clear that the fluctuations seen in the P_{B4_1} record are primarily associated with fluctuations in the integrated velocity in the upper water column. These fluctuations could represent either lateral changes in Gulf Stream position relative to the mooring or changes in Gulf Stream velocities, perhaps due to varying Gulf Stream transport. In the following, the P_{B4_1} fluctuations are presumed to be due to position changes, but it is acknowledged that part of the signal may result from transport variability.

2.3. Transport

Estimates of volume transport along and across the shelf were made for two rectangles or "boxes" in the horizontal along the continental shelf near Cape Hatteras. Box N (for north) was delimited to the north and south by mooring lines A and B out to moorings A3 and B3 (the shelf edge moorings, situated along the 60 m isobath). Mooring line D defined the easternmost boundary of box N. Box S (for south) was delimited by mooring lines B and C out to moorings B3 and C3 (shelf edge moorings along the 60 m isobath). No mooring line defined the easternmost boundary of Box S, so cross-shelf transport out of the box could not be directly calculated from data. Mooring line A crosses the shelf in an approximately E-W direction, Line B crosses the shelf at an angle of 15° clockwise from true east, and line C crosses the shelf at an angle of 43° clockwise from true east. Line D runs along the shelf edge at the 60 m isobath in a N-S direction.

Two aspects of the mean flow are evident in Figure 3. First, the flow into box N is predominantly convergent in the along-shelf sense and divergent across the shelf. Flow into box S also appears to be convergent along-shelf. Second, there is strong northeastward flow evident at the southeast corner of box N, because of the strong influence of the Gulf Stream at this location. Clearly, there are at least two types of flow processes occurring here. The first is the transient flow of Gulf Stream and shelf edge water across this corner, entering across the B line, and immediately exiting again across the D line. The second is the quantity of shelf and slope water that converges in the mean between lines A and B, which is exported somehow across line D. Figure 3 illustrates the problematic nature of isolating the components of along-shelf and cross-shelf shelf flow here relevant to the latter category from the transient Gulf Stream associated flux across this southeast corner. The situation is further complicated by the fact that the mechanisms of shelf water export probably depend on Gulf Stream variability as demonstated below and as indicated previously by *Churchill and Berger* [1998] and *Lillibridge et al.* [1990].

To help clarify this inherent difficulty, the flow was decomposed into along- and cross-shelf components. Along-shelf transports across mooring lines A, B, and C from the coast out to the shelf edge were calculated from the along-shelf flow components measured at the mooring locations, multiplied by some set of weights and summed across a mooring line. Both the along-shelf component of the flow and the weights to be applied could be determined in a variety of ways. For example, the along-shelf flow could be defined as the direction normal to the mooring line orientation, as the northward direction, or as the direction of the midwater column principal axis of variability at each mooring location. Correspondingly, the weights applied, calculated to represent the cross-sectional area of the flow that the point measurements of the moorings represent, could be calculated as mooring line cross-sectional area, that area projected onto an east-west vertical plane or that area projected locally onto a vertical plane perpendicular to the locally defined principle axis of the flow. Details of the resulting transport time series vary according to which method is selected. However, estimates of the along-shelf transport turn out to be fairly robust to these details of calculation, at least in terms of the results to be discussed below. The relevant analyses were conducted for each version of the transport calculations described above, and the primary results are similar. For that reason, the following discussions will focus on the method defining along-shelf flow as the northward component across lines A and B and as the flow normal to the mooring line orientation across line C. The advantage of this method is that for the box defined by mooring lines A, B, and D (box N) it is simply a calculation of flow into and out of a box with square corners, without the worry of correctly defining the direction of local isobaths. The disadvantage is that it may not properly resolve the transport into the physically relevant quantities of along- and across-shelf components. This is especially a problem at mooring B3, where the mean flows are large and northeastward. Mooring B3 presents an additional difficulty, in that the near-surface current meter records are incomplete and require a great deal of patching

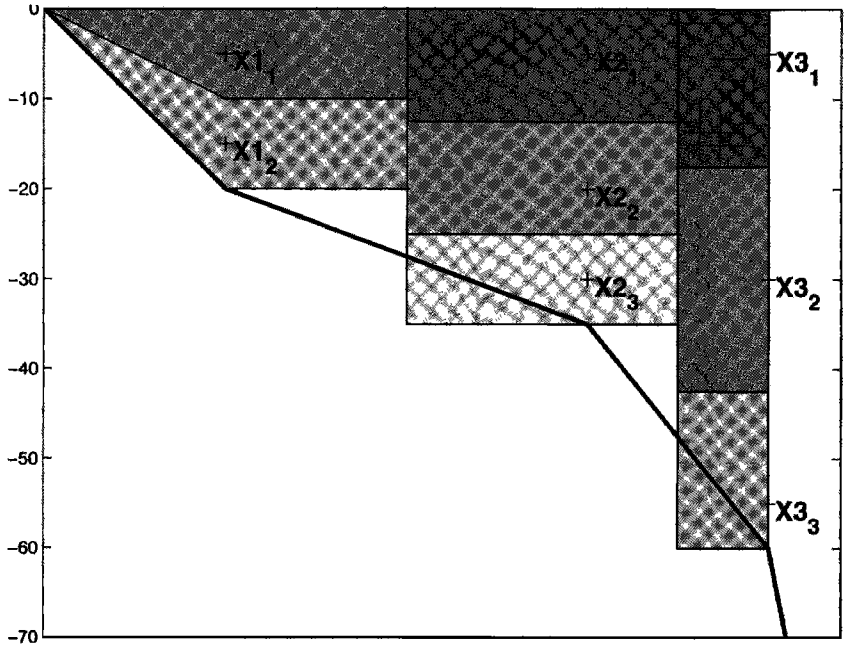

Figure 7. Schematic weight assignment for along-shelf transport calculations. The shaded area around each instrument location represents the portion of the mooring line cross-sectional area used as its weight in the transport calculations.

with data from deeper moorings or from nearby mooring locations (Figure 4). For that reason, along-shelf transports were also calculated without the inclusion of the shelf edge (A3, B3, and C3) moorings. These results are consistent with the full shelf calculations, as are midshelf transport results, calculated from A2, B2, and C2 moorings only. In the following, transports across the entire shelf will be reported. Spectral and emperical orthogonal function (EOF) results rely only on the midshelf component of transport. Parallel estimates for whole shelf transports show similar results.

Details of the along-shelf transport calculations are as follows: Current meter records were 48 hour low-pass filtered using a Hanning filter and subsampled to 1 day intervals. Gaps in the data were filled by using data from the same mooring location when possible. Nearby moorings from the same mooring line were used when no information was available at the same mooring location. For example (see Figure 4), gaps in the $A2_1$ and $A2_3$ northward and eastward component current meter records were filled with $A2_2$ records, with means and standard deviations adjusted to match the existing records. Gaps in the $B3_1$ records were filled first with $B3_2$ records, then with $B3_3$ records, and finally, with $B2_1$ records, each with means and standard deviations adjusted to match the existing $B3_1$ records. $B3_2$ record gaps were filled first with $B3_3$ records, then with $B2_2$ records. True north was defined as the along-shelf direction for mooring lines A and B, while the direction normal to the mooring line was used as the along-shelf direction for mooring line C. The weights for the transport calculations were calculated as illustrated by the shaded areas in Figure 7 and are listed in Table 1, rounded to the nearest m^2. A more sophisticated weighting scheme could have been devised, taking into account the average bottom slope between mooring locations. While the coarsely defined bottom weights used here will affect the absolute transport and convergence numbers to some degree, they do not affect the major results concerning transport and convergence variability or the coherence of those variables with the relevant forcing functions. For mooring lines A and C, Table 1 values are the areas represented by the schematic in Figure 7. For mooring line B they are those areas projected onto an east-west vertical plane. The resolution provided by just three mooring locations, with at best three mooring packages in the vertical at each location, will obviously miss finer-scale features in the transport on the shelf. For example, the transport carried by the narrow jet that is known to exist along the Mid-Atlantic Bight shelf edge [*Gawarkiewicz et al.*, 1996; *Linder and Gawarkiewicz*, 1998] would be poorly represented in these calculations. It is hoped that the long timescales

Table 1. Weights Assigned to Velocity Measurements for Along-Shelf Transport Calculations [a]

Line	A	B	C
Mooring 1_1	2.59061	1.71194	1.57189
Mooring 1_2	2.76089	2.01353	1.73735
Mooring 2_1	4.49103	2.34854	2.63349
Mooring 2_2	4.49103	2.34854	2.63349
Mooring 2_3	3.59283	1.87883	2.10679
Mooring 3_1	2.35412	0.91327	1.23801
Mooring 3_2	3.36303	1.30467	1.76859
Mooring 3_3	2.35412	0.91327	1.23801

[a] Weights are in $10^5 \times m^2$

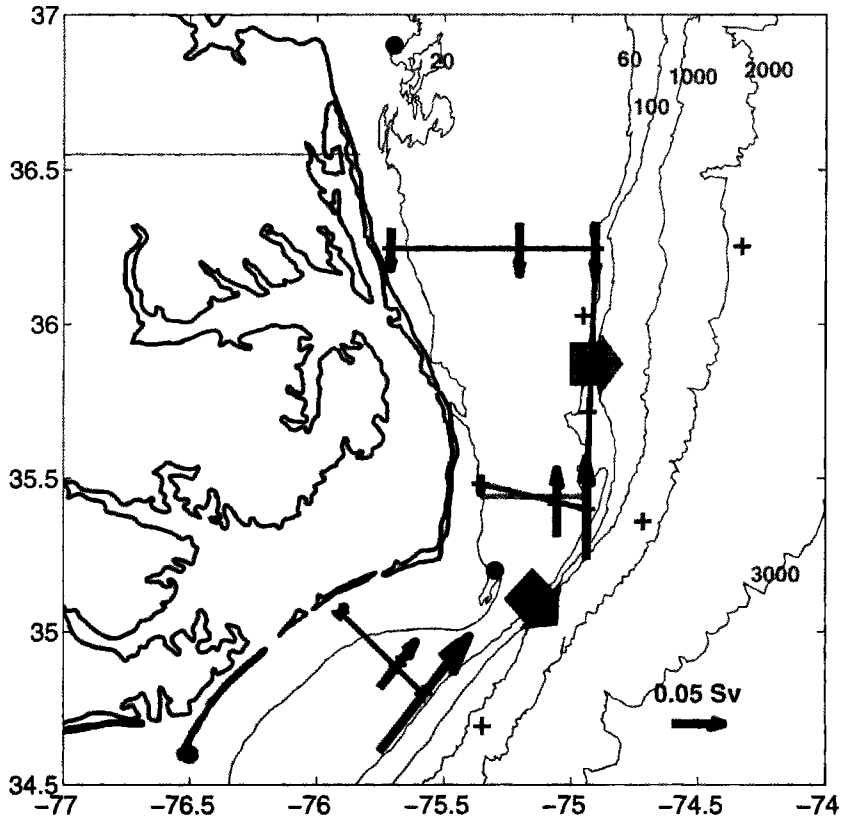

Figure 8. Mean along-shelf transport at shelf mooring locations. Offshore transport arrows are implied by along-shelf convergence and are not drawn to scale. Mooring locations (pluses) and C-MAN wind data stations (solid circles) are shown.

of the processes highlighted in this study will mitigate this shortcoming to some degree. Bottom instruments at C2 and C3 showed suspect rotations, so tranport calculations for line C are briefly reported but are not held in high regard.

Cross-shelf transport, unlike along-shelf transport, is quite sensitive to the definition of the offshore direction, in terms of whether or not horizontal divergence of the volume transport sums to zero over some reasonable time frame. The only case for which an approximate balance was calculated between along-shelf convergence of volume and cross-shelf divergence was for the simple box: along-shelf was defined as N-S, and off-shelf was defined as E-W. Fortunately, since horizontal divergence must sum to zero over some reasonable time frame, the cross-shelf transport calculations are largely redundant: if along-shelf convergence is known, then in essence, cross-shelf divergence is also known. Details at short timescales of how that divergence is accomplished in the spatial domain are not necessarily known, however. In the following, cross-shelf transport calculations from mooring line D data are not reported directly. Instead, cross-shelf transports are inferred from the along-shelf divergence, assuming no net flow through the boundaries, no appreciable change in sea surface height, and continuity. The assumption of negligible sea surface height change at the periods under scrutiny here is addressed in section 6.

3. Mean Transport and Short-Term Variability

Mean along-shelf transport into boxes N and S is convergent, with mean flow across line A to the south, and mean northward flow across line C exceeding mean northward flow across line B (Figure 8). On the daily timescale flow into box N is convergent for ~90% of the experiment time (Figure 9). The flow is highly correlated across lines A and B with demeaned along-shelf transport showing highly coherent fluctuations. The along-shelf transport fluctuations are primarily wind-driven, with winds leading by less than half a day across a wide frequency band (Figure 10). The convergence in both boxes is robust to wind direction and the direction of those wind-driven transports. That is, transport variability on the shelf across lines A and B follows wind variability: northward winds correspond to northward fluctuations in transport on the shelf, and southward winds correspond to southward fluctuations in transport on the shelf, but in either case the along-shelf transport into box N is convergent 90% of the time. This provides reassurance that the net convergence seen is not a function of the weighting scheme but rather is a feature of the flow itself. The along-shelf convergence in box N implies a mean offshore transport of about 0.24 Sv (0.19 Sv standard devi-

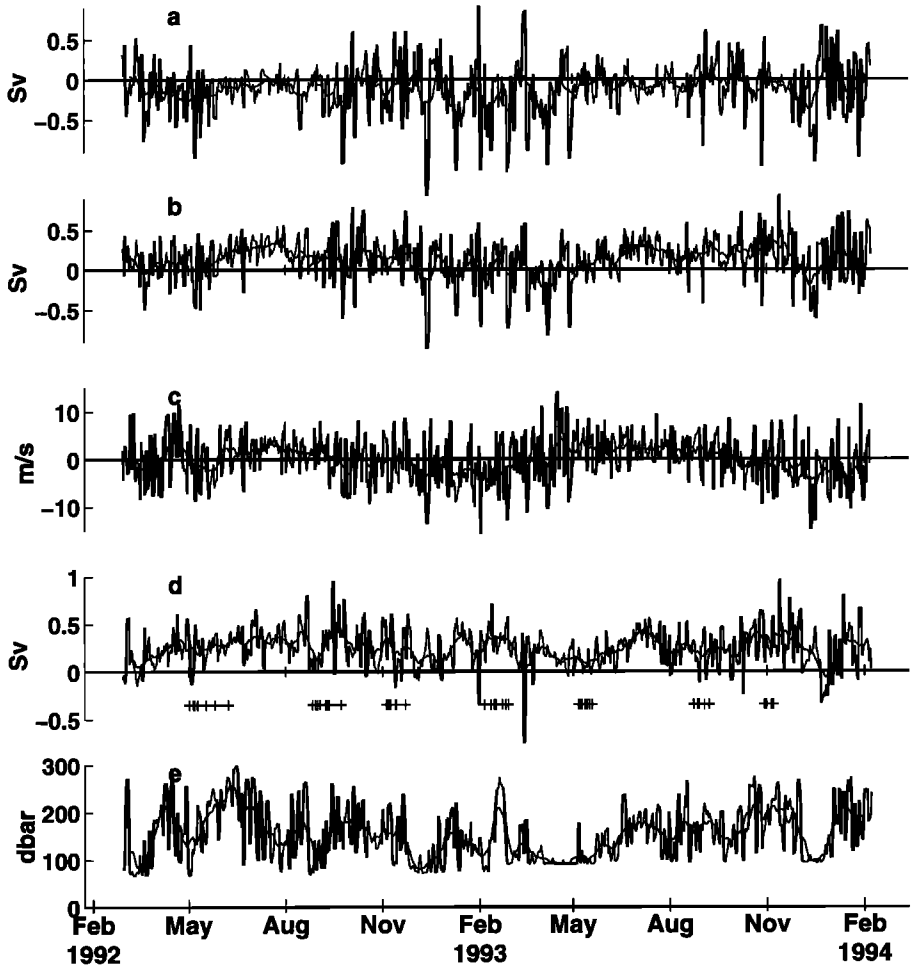

Figure 9. Selected 48 hour low-passed and 15 day low-passed time series: (a) northward transport across mooring line A, (b) northward transport across mooring line B, (c) along-shelf wind at CHLV2, (d) along-shelf convergence (B-A transports), and (d) the 100 m pressure record at mooring B4, (P_{B4_1}). P_{B4_1} serves as a proxy for Gulf Stream offshore position, with higher values corresponding to more shoreward stream positions. Times of float deployment during the experiment are plotted below the transport convergence panel (pluses for start days and end days, with a solid line between).

ation) (1 Sv=10^6 m^3 s^{-1}). It should be stressed that this number is not a reliable quantitative estimate of shelf water export for this region, depending as it does on the placement of the offshore boundary of the box, not on the identification of specific water types exiting there. It is reported here simply to illustrate that the magnitude is in keeping with other estimates of water expected to be leaving the system here (see *Churchill and Berger* [1998] for shelf water export estimates from this data set and a comparison with previously estimated values). If the transports across lines A and B are broken down into components, another interesting feature emerges. Mean transports at A1, A2, A3, and B1 are equatorward, in the mean, while transports at B2 and B3 are poleward. The flow is convergent across the entire shelf in box N: shoreward of the 25 m isobath, as represented by the B1−A1 transports; between the 25 and 45 m isobaths, as represented by the B2−A2 transports; and between the 45 and 60 m isobaths, as represented by the B3−A3 transports.

Along-shelf winds here are slightly divergent in the mean. The transport convergence is not well correlated with the wind (Figure 11) or the wind convergence (not shown). Instead, along-shelf convergence is highly coherent with the Gulf Stream position proxy over several frequency bands (Figure 11). These cross spectra will be examined in detail in section 5.

Along-shelf flow into box S is also primarily convergent but less robustly so than in box N. Here convergence is seen 64% of the experiment time. Velocities across line C are poleward in the mean, are highly correlated with flow across lines A and B, and are wind-driven (not shown). The observed convergence requires a mean offshore transport of 0.15 Sv; however, the suspect rotations on the line C outer bottom instruments make this result of limited value. Here, too, the convergence is robust to wind and velocity fluctuation direction, lending credence to the qualitative result.

4. Long-Period Along-shelf Convergence

The mean along-shelf convergence of 0.24 Sv into box N implies a corresponding mean offshore transport across

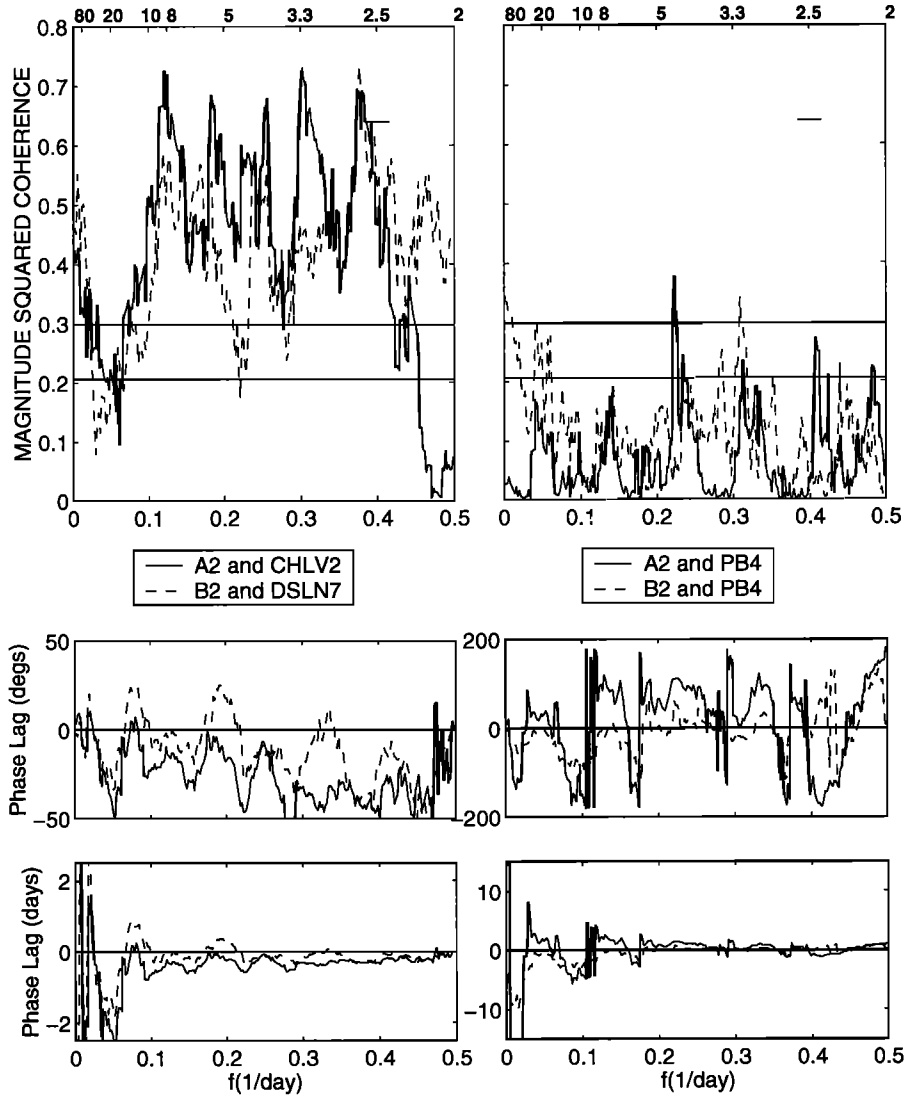

Figure 10. Cross spectra between transports and possible forcing functions: (left) cross spectra between northward transport at midshelf mooring A2 and CHLV2 along-shelf wind (solid line) and between along-shelf transport at midshelf mooring B2 and DSLN7 along-shelf wind (dashed line), (right) cross spectra between northward transport at midshelf mooring A2 and P_{B4_1} (solid line) and between along-shelf transport at midshelf mooring B2 and P_{B4_1} (dashed line), (top) magnitude squared coherence (drawn to the same scale), (middle) the phase lag in degrees, and (bottom) the phase lag in days, converted from degrees by $\theta_{day} = \theta_{deg}/(f360)$, where f is frequency. Positive phase lags indicate that the first quantity in the pair leads the second. Horizontal lines in the top panels show the 99% and 95% confidence levels.

mooring line D of the same magnitude. Of the total mean accumulation in box N, ~33% is accounted for by equatorward flow across line A, and ~66% is accounted for by poleward flow across line B. The magnitude of the convergence and its partitioning between flow across line A and line B varied in time in an interesting way. In order to investigate this, transports were very low passed with 30 and 120 day rectangular filters. The 120 day filtered time series will be considered first (Figure 12).

There is a strong annual signal in transport across lines A, B, and C. The flow across lines A and B lags the low-passed along-shelf wind at Diamond Shoals by ~1-2 months. The annual fluctuations appear to be primarily in phase between lines A and B, with local maxima in August-September and reaching minima in February-March. During summer, large poleward transport across line B outweighs (by a factor of about 2) the contribution from equatorward flow across line A, which is at its annual minimum in magnitude then. During winter, equatorward flow across line A accounts for almost 100% of the estimated convergence, with poleward flow across line B falling to near or below zero. The strong, approximately annual signal in flow across both lines A and B results in a signal in the along-shelf convergence that is not annual (Figure 12d). The convergence during summer of 1993 shows a broad, poorly defined peak, whose apex appears to be something between 14 and 16 months later than the peak in the preceding summer. The winter convergence averages about two-thirds the magnitude of the sum-

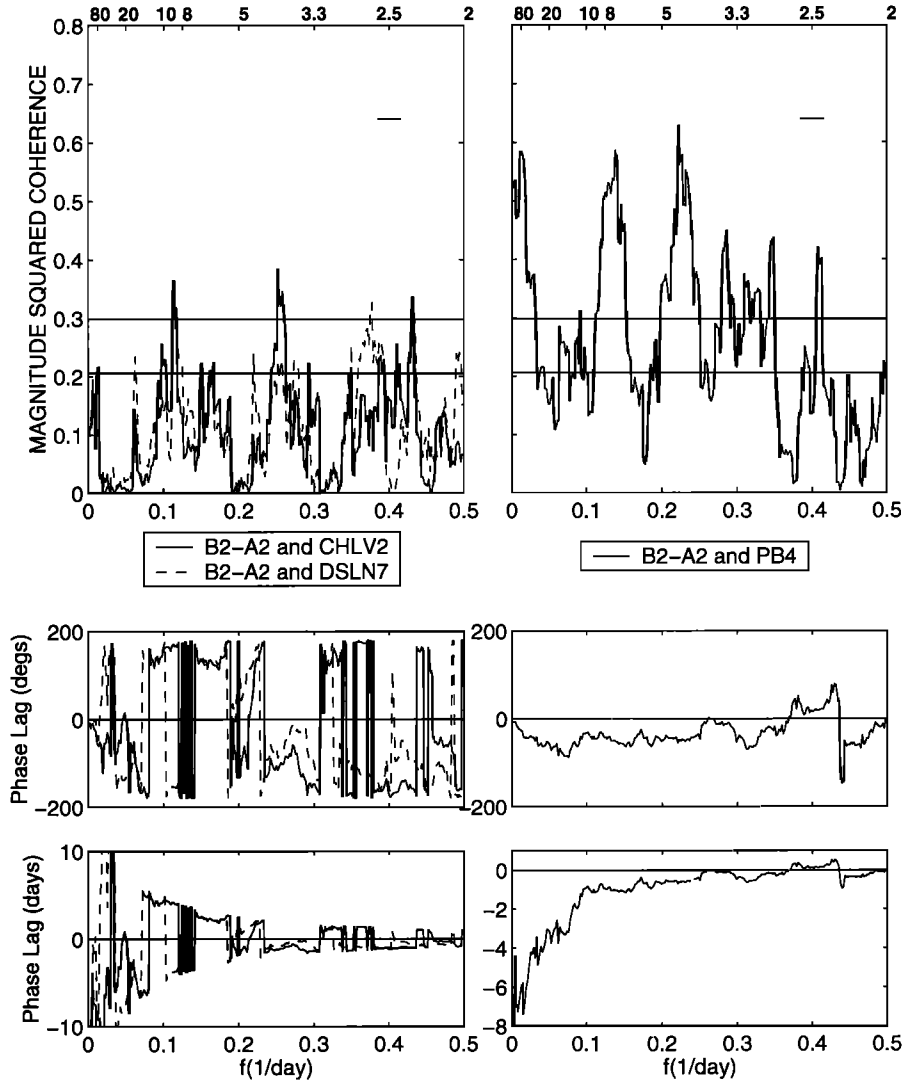

Figure 11. Cross spectra between transport convergence and forcing functions: (left) cross spectra between along-shelf transport convergence (B2-A2 transports) and CHLV2 along-shelf wind (solid line) and between along-shelf transport convergence and DSLN7 along-shelf wind (dashed line), (right) cross spectra between along-shelf transport convergence and P_{B4_1} (solid line), (top) magnitude squared coherence (drawn to the same scale), (middle) the phase lag in degrees, and (bottom) the phase lag in days, converted from degrees by $\theta_{day} = \theta_{deg}/(f360)$, where f is frequency. Positive phase lags indicate that the first quantity in the pair leads the second. Horizontal lines in the top panels show the 99% and 95% confidence levels.

mer peaks, which are each near 0.3 Sv. Poleward flow across line C also shows a strong annual signal (not shown), the peaks of which lead those at line B by ~30-60 days. The transport minimum across line C during winter is quite broad and does not appear to lead that at line B. Poleward transport across line C exceeds that across line B at almost all times during the year. The resulting convergence shows a semiannual signal (not shown). In box S the late winter convergence peak is of approximately the same magnitude or greater than the summer values.

The 120 day filtered time series of along-shelf winds show a strong annual signal, with equatorward wind in winter, and poleward wind in summer (Figure 12). The turning of the wind with season has been noted before [*Blanton et al.*, 1985; *Werner et al.*, 1999]. Despite significant variability in the winds on short timescales this seasonal signal is quite robust (Figure 13a) and results from the annual variability in predominant wind direction and magnitude (Figure 13b). Pressure fluctuations at mooring B4, the proxy for Gulf Stream offshore position, also show a long-period signal (Figure 12), but this does not appear to be an annual signal as the broad peaks seem more consistent with a 14-16 month periodicity.

The 30 day low-passed transports illuminate some additional features of the along-shelf convergence at Cape Hatteras (Figure 14). Predominant in these plots are strong, several-month period fluctuations, from 30-90 days up to ~5 months. The 30 day low-passed winds show less evi-

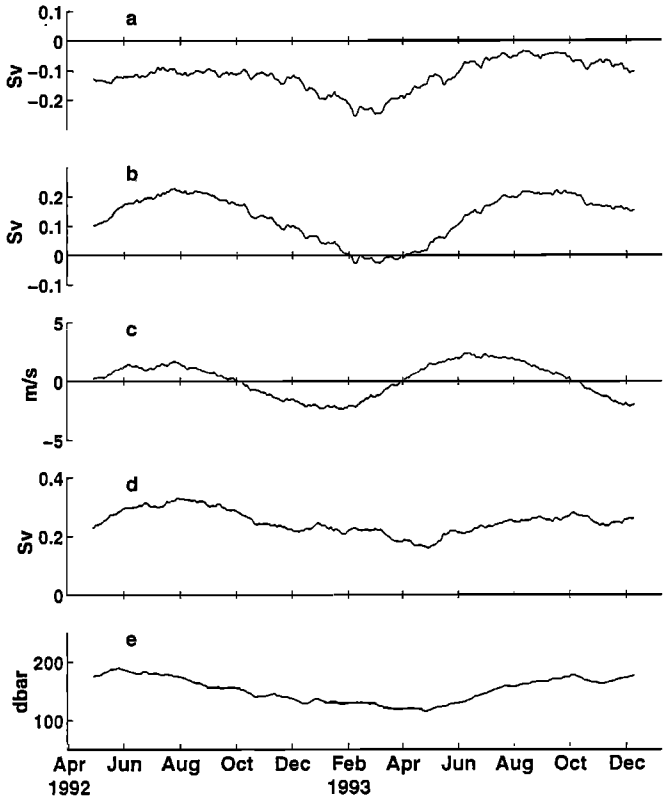

Figure 12. Selected 120 day low-passed time series: (a) northward transport across mooring line A, (b) northward transport across mooring line B, (c) along-shelf wind at CHL, (d) along-shelf convergence (B-A transports), and (e) the uppermost pressure record at mooring B4 (P_{B4_1}). P_{B4_1} serves as a proxy for Gulf Stream offshore position, with higher values corresponding to more shoreward stream positions.

dence of this signal. Conversely, the 30 day low-passed pressure record at mooring B4 shows a strong 30-90 day signal, which is in phase with the transport convergence estimates. Note especially the local minima in transport convergence and Gulf Stream position during the Decembers of 1992 and 1993 and in late April of 1993. Note also a 4-5 month periodicity in local maxima in Gulf Stream position, with peaks in June and October of 1992 and March, July, and November of 1993. Corresponding peaks show up clearly in the transport convergence time series in late 1992 and 1993 but are not clear in early 1992.

5. Forcing

Cross spectral and EOF analyses were used to assess the relationships apparent in the transport, transport convergence, wind, and Gulf Stream position time series. For the cross spectral analyses the multitaper method was used in order to get the most information possible about the long period fluctuations. The more typically used Welch's overlapped segment averaging (WOSA) method proceeds by dividing each time series into overlapping segments, tapering each segment with an identical filter to reduce bias, running the spectral analysis on each segment, and then averaging the results over all segments by frequency to reduce variance [*Percival and Walden*, 1993]. The initial subdivision in the WOSA method reduces the information available for the long-period variability. The multitaper method instead uses a series of different tapers on the complete time series to reduce bias, with spectral analysis on each differently tapered version of the data, averaged over all realizations to reduce variance [*Percival and Walden*, 1993]. Without any series length reduction, more information is preserved about the longer-period variability. Using successively more tapers reduces variance of the final averaged spectral estimate but introduces increasing bias in the spectral estimates. If the investigator is content with high bandwidth (poor frequency resolution), it is possible to get very high reduction of variance with very little introduction of bias. For the present case a duration times the half-bandwidth product of 8 was chosen, allowing for a total of 15 discrete prolate spheroidal sequences to be used as tapers. The resulting variance is quite low, as are the 95 and 99% confidence threshold levels for coherence.

Cross spectra were calculated between various combinations of representative transports, transport convergences, winds, and P_{B4_1} (the Gulf Stream position proxy). The midshelf component of transports and transport convergences were used instead of the shelf-wide estimates for two reasons. First, processes important shelf wide should certainly show up in relationships derived for the midshelf components. The inclusion of the shelf edge transport components might unduly skew the results toward shelf edge processes.

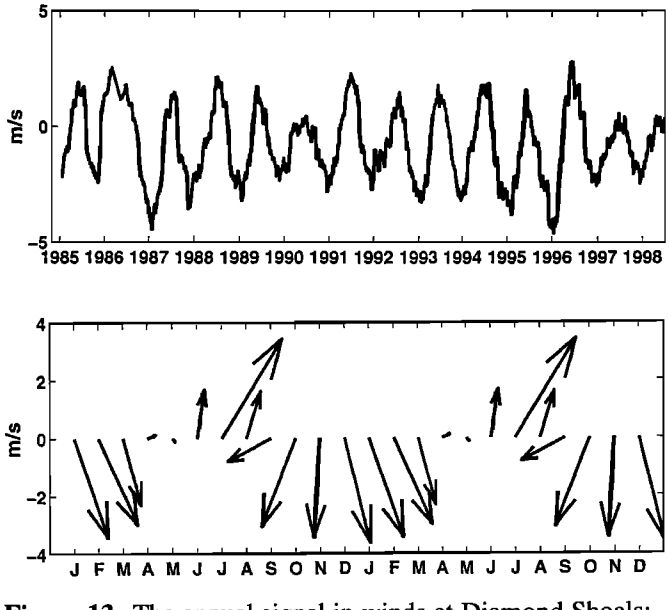

Figure 13. The annual signal in winds at Diamond Shoals: (top) 120 day low-passed northward velocities from C-MAN station DSLN7 for 1985 through mid-1998 and (bottom) stickplot of the average seasonal signal repeated for 2 years. This stickplot time series was calculated as monthly averages over all values for each month over the years 1986-1995. These were years with fairly continuous, good quality data in both vector components.

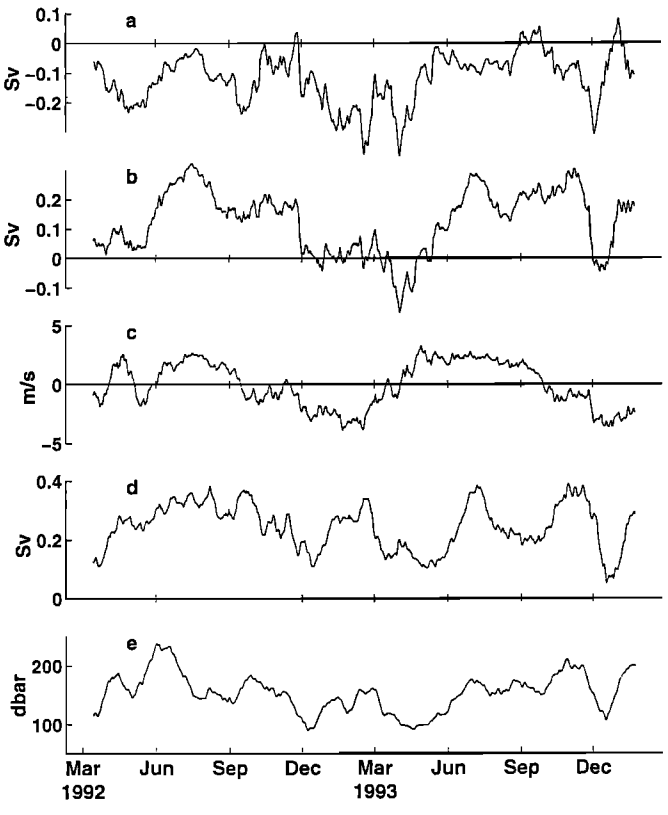

Figure 14. Selected 30 day low-passed time series: (a) northward transport across mooring line A, (b) northward transport across mooring line B, (c) along-shelf wind at CHLV2, (d) along-shelf convergence (B-A transports), and (e) the uppermost pressure record at mooring B4 depth (P_{B4_1}). P_{B4_1} serves as a proxy for Gulf Stream offshore position, with higher values corresponding to more shoreward stream positions.

In addition, the B3 mooring, in particular, was problematic, as discussed in section 2.3, by its close proximity to the Gulf Stream and in the extreme gappiness of its upper sensor (Figure 4). It was therefore advantageous not to make the spectral results contingent on the quality of the B3 data. In fact, spectral estimates calculated using the shelf-wide estimates of transport (not shown) show similar results to those discussed below, despite the above concerns. Further spectral analysis using only the relatively complete middepth sensors from the midshelf moorings ($A2_2$ and $B2_2$) show results that are clearly consistent with those discussed below.

Cross spectra between CHLV2 wind and A2 transport or between DSLN7 wind and B2 transport show high coherence across a broad range of frequencies from 0.075 to 0.425 d^{-1} (~2-20 day periods), with winds leading transports by less than a half a day (Figure 10). Coherences between transport at A2 or B2 and the Gulf Stream position proxy are low across almost all frequencies (Figure 10). Conversely, cross spectra between CHLV2 or DSLN7 wind and transport convergence show low coherence across most frequencies, with singular peaks at ~0.12 day^{-1} (9 day period) (Figure 11). Coherence between transport convergence and the Gulf Stream position proxy is high in several broad frequency bands: the low frequencies between 0 and 0.03 d^{-1} (30-512 days), between 0.1 and 0.15 d^{-1} band (7-9 days), and between 0.2 and 0.25 d^{-1} band (4-5 days), and a variety of narrow peaks from between 0.28 and 0.42 d^{-1} band (2.4-3.5 days) (Figure 11). The 7-9 day periods are typical of Gulf Stream meanders in this region [*Webster*, 1961; *Brooks and Bane*, 1981, 1983], while *Glenn and Ebbesmeyer* [1994b] found a 4.6 day periodicity in Gulf Stream meanders right at Cape Hatteras. For the high coherence bands between 3.5 and 9 day periods, the Gulf Stream proxy time series leads along-shelf transport convergence by 0.5-1 day. The lowest frequency band of high coherence (30-512 days) is characterized by the Gulf Stream proxy leading along-shelf convergence on the average of 5 days. Coherence between wind convergence and midshelf transport convergence is low, with one significant peak at about the 9 day period (not shown).

EOF analyses were performed on selected daily time series for the period February 28, 1992, to February 7, 1994, to gain additional understanding of the low-frequency variability seen in the transports and transport convergences (discussed in section 4). Midshelf along-shelf velocity, transport, and transport convergence time series were run with potential "forcing functions" of along-shelf wind, along-shelf divergence of wind, and P_{B4_1} (Gulf Stream position proxy). Three specific cases will be examined below, with further remarks reflecting a battery of related cases as needed.

Case 1 used transport at mooring A2, CHLV2 along-shelf wind, and P_{B4_1}. This represents transport between approximately the 23 and 48 m isobaths on the midshelf. Table 2 indicates that transport at A2 and wind forcing have much in common, with all of their variance in modes 1 and 3, while P_{B4_1} is practically all in mode 2, with little variability in modes 1 and 3. This suggests that variability in transport at A2 is dominated by wind effects. A companion case using velocity at $A2_2$ (20 m depth) instead of A2 transport shows essentially identical partitioning.

Case 2 used along-shelf transport at mooring B2, DSLN7 along-shelf wind, and the B4 pressure record. Here there is no clear separation between wind and Gulf Stream forcing nor are any of the resulting modes clearly identifiable as primarily wind and Gulf Stream forcing (Table 3). This suggests that closer to Cape Hatteras, both wind and Gulf Stream effects have direct influence on the midshelf along-shelf current. This is not surprising given the proximity of the Gulf Stream and the narrowness of the shelf in this loca-

Table 2. EOF Eigenvectors and Eigenvalues for Line A Transport, Wind, and Gulf Stream Position

	Mode 1	Mode 2	Mode 3
TR_{A2}	0.7070	0.0092	0.7072
V_{CHLV2}	0.7068	0.0235	-0.7070
GS_{pr}	0.0231	-0.9997	-0.0101
Evals	1.5459	0.9998	0.4544
	(52%)	(33%)	(15%)

TR_{A2} is along-shelf transport at mooring A2; V_{CHLV2} is along-shelf wind at C-MAN station CHLV2; GS_{pr} is the pressure from the 100 m depth instrument package at mooring B4, used here as a proxy for Gulf Stream distance offshore; Evals are eigenvalues.

Table 3. EOF Eigenvectors and Eigenvalues for Line B Transport, Wind, and Gulf Stream Position

	Mode 1	Mode 2	Mode 3
TR_{B2}	0.7169	-0.0251	0.6967
V_{DSLN7}	0.5934	0.5465	-0.5909
GS_{pr}	0.3659	-0.8371	-0.4067
Evals	1.6197	1.0365	0.3438
	(54%)	(35%)	(11%)

TR_{B2} is along-shelf transport at mooring B2; V_{DSLN7} is along-shelf wind at C-MAN station DSLN7; GS_{pr} is the pressure from the 100 m depth instrument package at mooring B4, used here as a proxy for Gulf Stream distance offshore; Evals are eigenvalues.

tion. Recall, however, that the cross spectra discussed above showed B2 transport well correlated with winds and poorly correlated with P_{B4_1}. EOF analysis cannot accurately define the relationship among variables for which significant lags apply.

Case 3 used along-shelf convergence between A2 and B2, CHLV2 along-shelf wind, and P_{B4_1}. This represents convergence between approximately the 23 and 48 m isobaths on the midshelf. Table 4 indicates that transport convergence on the midshelf and Gulf Stream position have much in common, with all of their variance in modes 1 and 3, while winds are practically all in mode 2, with little variability in modes 1 and 3. This suggests that variability in transport convergence is dominated by Gulf Stream forcing. Similar results are obtained using DSLN7 winds or the unrotated northward component of winds at DSLN7 or CHLV2.

Both the cross spectral analyses and the EOF analyses illustrate that fluctuations in transport are closely tied to wind field variability across a wide band of frequencies (2-20 days), probably representing the weather band, despite high energy variability in the Gulf Stream at similar periods. Variability in along-shelf convergence, on the other hand, is poorly correlated with wind or wind convergence variability. Instead, transport convergence appears to be tied to variability in Gulf Stream position, with peaks in convergence associated with more onshore locations of the Gulf Stream. Since the transport convergence results from contributions at both line A and line B, it is unlikely that the convergence results simply as a consequence of increasing flow across line B during nearshore Gulf Stream events. This topic is taken up again in section 8. A more likely hypothesis is that the Gulf Stream is directly influencing cross-shelf export processes along the outer boundary of box N. By continuity, modulation of cross-shelf transport would require compensating along-shelf convergence. This is consistent with P_{B4_1} fluctuations leading transport convergence fluctuations, as seen in the cross spectral analyses.

6. Along-Shelf and Cross-Shelf Imbalances

Direct calculations of the cross-shelf transport from the mooring data along line D were not entirely consistent between methods of defining the cross-shelf direction and so did not provide consistent estimates of the balance between along-shelf convergence and cross-shelf divergence. However, cross-shelf divergence estimates were of approximately the same magnitude as the along-shelf convergence estimates, such that most of the continuity requirement could be expected to be satisfied by the two horizontal transport components. However, there is no reason to expect that such a balance holds uniformly over all timescales. In fact, transport mismatches of up to 10% are suggested by these admittedly large error estimates. If 0.24 Sv net mean transport enters the box across lines A and B and only 90% leaves the box over a given day, the net sea level change required over the area of the box (5.890×10^3 km^2) is on the order of a half meter, if uniformly distributed over the box. For that reason, coastal sea level was investigated at Duck, North Carolina, a location within the study site (see Figure 1), to determine its relationship to the long-period signals discussed above.

The sea level records were corrected for the inverted barometer effect using nearby atmospheric pressure corrected to sea level [*Blanton*, 2001]. Short gaps (<6 hours) were filled using a spline technique. The data were 40 hour low-pass filtered and decimated to 6 hourly intervals. The daily (48 hour low-passed) wind, transport, and Gulf Stream position proxy data were interpolated to 6 hourly values for consistency. Cross spectral analysis using the multitaper method indicates strong coherence between A2 transport and sea level at Duck and between CHLV2 winds and Duck sea level across a wide frequency band (Figure 15). Poleward wind and along-shelf transport are correlated with low sea level at Duck, while equatorward wind and along-shelf transport are correlated with high sea level. (Note that the sea level records have been multiplied by -1 for these cross spectra to simplify interpretation of phase lags.) Coastal sea level is commonly understood to respond to along-shelf winds through cross-shelf Ekman transport, convergence or divergence at the coastline, and the development of a geostrophically balanced along-shelf current [*Csanady*, 1982]. Y. Y. Kim et al. (On the mass and salt budgets for a region of the continental shelf in the southern Mid-Atlantic Bight, submitted to *Journal of Geophysical Research*) also found coastal sea level to be well correlated with winds and transport in this location. Sea level is far less coherent with either Gulf Stream position or transport convergence, except for a band

Table 4. EOF Eigenvectors and Eigenvalues for Transport Convergence, Wind, and Gulf Stream Position

	Mode 1	Mode 2	Mode 3
CON_{B2-A2}	0.6988	-0.1470	-0.7001
V_{DSLN7}	-0.1132	-0.9890	0.0947
GS_{pr}	0.7063	-0.0131	0.7077
Evals	1.4642	0.9982	0.5376
	(49%)	(33%)	(18%)

CON_{B2-A2} is the convergence in along-shelf transport at midshelf (B2 transport-A2 transport); V_{DSLN7} is along-shelf wind at C-MAN station DSLN7; GS_{pr} is the pressure from the 100 m depth instrument package at mooring B4, used here as a proxy for Gulf Stream distance offshore; Evals are eigenvalues.

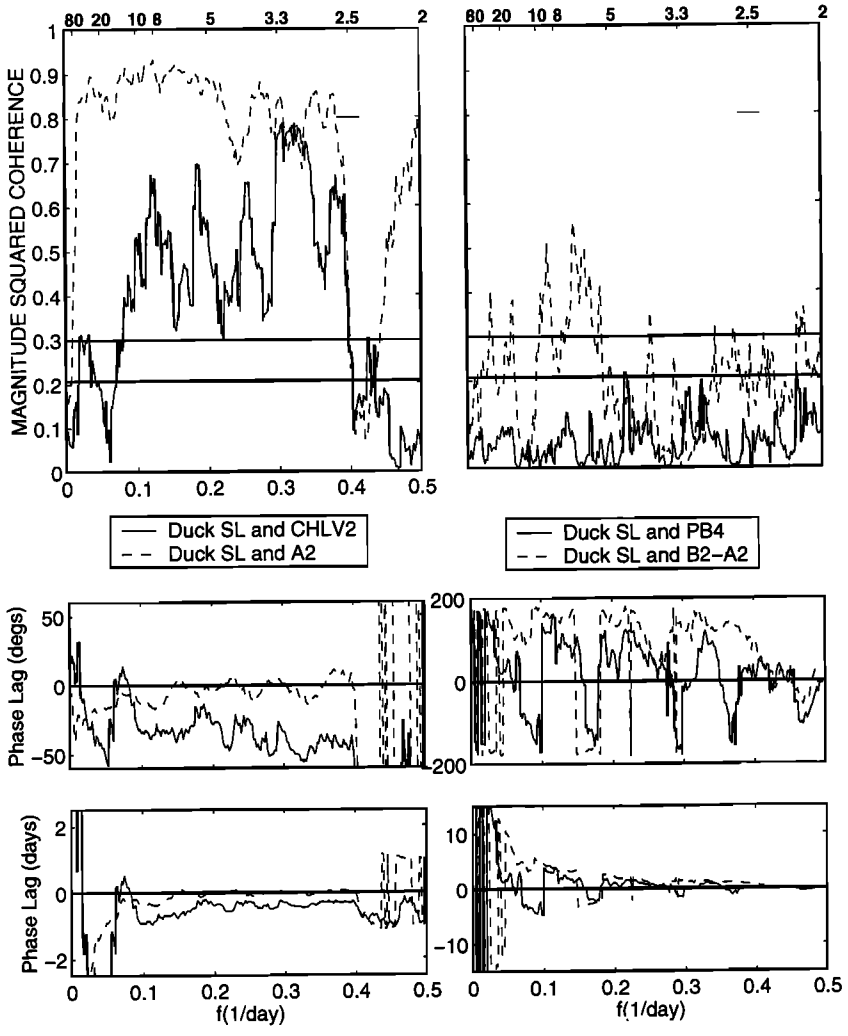

Figure 15. Cross spectra between coastal sea level, transport, winds, and Gulf Stream position proxy: (left) cross spectra between corrected sea level at Duck, North Carolina ($\times -1$) and along-shelf wind at CHLV2 (solid line) and between corrected sea level at Duck ($\times -1$) and northward transport at midshelf mooring A2 (dashed line), (right) cross spectra between corrected sea level at Duck, North Carolina ($\times -1$) and P_{B4_1} (solid line) and between corrected sea level at Duck ($\times -1$) and midshelf along-shelf transport convergence (B2-A2 transports) (dashed line), (top) magnitude squared coherence (drawn to the same scale), (middle) the phase lag in degrees, and (bottom) the phase lag in days, converted from degrees by $\theta_{day} = \theta_{deg}/(f360)$, where f is frequency. Positive phase lags indicate that the first quantity in the pair leads the second. Horizontal lines in the top panels show the 99% and 95% confidence levels.

of low peak correlation between convergence and sea level near 0.4-0.5 at 12-5 days. This implies that the compensation for long-period along-shelf convergence is almost completely accomplished by cross-shelf divergence, as no systematic variability in sea level height with convergence is evident. Conversely, although wind-forced transport variability dominates sea level variability at weekly to biweekly timescales, some non-Gulf Stream-related convergence may play a part.

These sea level results cast some doubt on whether the Gulf Stream influence on cross-shelf transport seen in the midshelf and shelf-wide results extends to the nearshore regime. (The shelf-wide transports and convergences are dominated by the midshelf records.) To explore this question, along-shelf transports at moorings B1 and A1 (both on the 20 m isobath) were examined. Clearly, the nearshore along-shelf transports are highly correlated with the along-shelf wind (Figure 16), just as the midshelf transports were. Transport is primarily convergent, despite more frequent divergent events than are seen in the midshelf and shelf-wide records and the fact that mean transport is southward at the 20 m isobath across both lines A and B (Figures 16 and 3). However, the nearshore transport convergence bears less resemblance to the Gulf Stream proxy than did the shelf-wide time series (compare Figures 9 and 16). Cross spectra between this nearshore transport convergence (B1-A1) and CHLV2 and DSLN7 alongshore winds and the Gulf Stream proxy indicate low correlation at all frequencies between the Gulf Stream position proxy and nearshore along-shelf convergence and moderately high significant values of co-

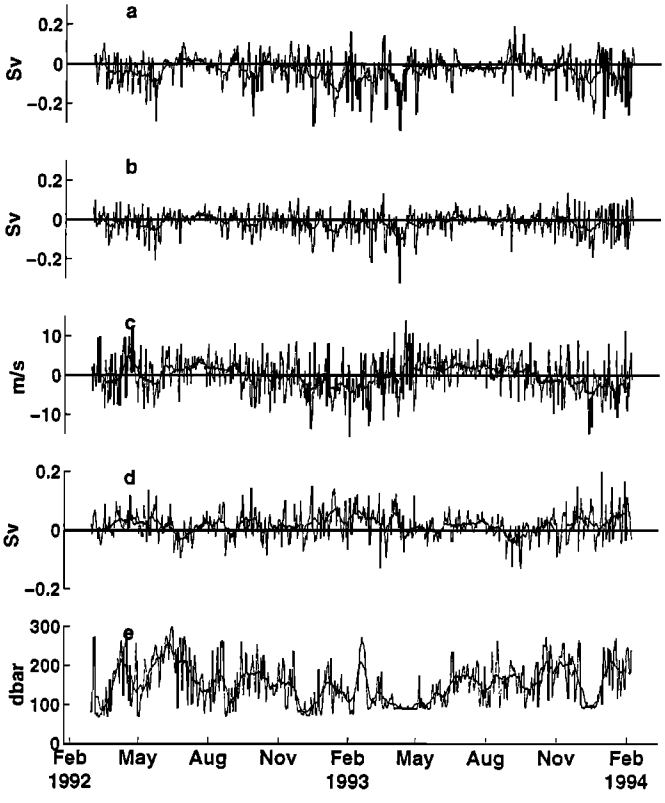

Figure 16. Selected 48 hour low-passed and 15 day low-passed time series: (a) northward transport at mooring A1, (b) northward transport at mooring B1, (c) along-shelf wind at CHLV2, (d) nearshore along-shelf convergence (B1-A1 transports), and (e) the uppermost pressure record at mooring B4 (P_{B4_1}). P_{B4_1} serves as a proxy for Gulf Stream offshore position, with higher values corresponding to more shoreward stream positions.

herence between wind and near-shore along-shelf convergence at ~9-10 and 2-2.5 day period bands (Figure 17). This coherence between wind and along-shelf convergence nearshore exceeds that seen on the midshelf but is lower than the correspondence seen at midshelf between transport convergence and the Gulf Stream position at almost all frequencies. Clearly, one of the primary results of this paper (that along-shelf convergence is highly correlated with Gulf Stream distance offshore, and poorly correlated with along-shelf winds) does not apply on the inner shelf, as represented by these 20 m isobath transport calculations.

7. Occasional Along-shelf Divergence

Despite predominantly convergent along-shelf flow near Cape Hatteras, especially between lines A and B, episodes of along-shelf divergence do occur, accounting for 10% of the experiment time. These occasions are seen as the negative spikes in the convergence estimates (Figure 9). Most persist for very short periods, a day or two, while one particularly striking example in December 1993 lasted 8 days. Along-shelf divergence implies cross-shelf convergence, i.e., shoreward flow across the middle to outer shelf. The magnitudes of the implied onshore transports would require shoreward velocities of $O(0.02\ \mathrm{m\ s^{-1}})$ if uniform flow across the entire offshore boundary of boxes N or S were presumed. Shoreward velocities confined to the smaller cross sections of specific portions of the water column would require commensurately higher velocities. Given the narrow shelf widths near Cape Hatteras, such magnitudes of specific water parcels are not insignificant. Evidence of such shoreward flow might be expected to appear in the data, either in the moored current meter records or in the drifter paths. In fact, the E-W component of flow at several moorings ($A1_1$, $A1_2$, $A2_2$, $A2_3$, $D1_3$, and at all depths at D2) showed mean westward flow of a few cm s^{-1} during divergent days, and for 2 days preceding divergence, despite record-long eastward mean flow at these locations. (Standard deviations of onshore velocity during along-shelf divergent days were larger than the means over those days and larger than the change in means from convergent to divergent day pools but are consistent with record-long standard deviations.) In the drifter data from this experiment, *Berger et al.* [1995] found no convincing evidence of onshore flow. A few drifter deployments coincided with single-day divergence in box N. Unfortunately, during the strong box N divergence events (the 3 day event in March 1993 and the 8 day event of December 1993) none of the drifters were under surveillance on the shelf.

The along-shelf divergent days in box N coincided with days when the Gulf Stream was located relatively far from shore and usually with northward transport along-shelf. Satellite imagery of AVHRR SST for the period December 20, 1993, to January 1, 1994, helps illustrate what may have occurred (Figure 18). During this time, along-shelf flow on the shelf was northward and divergent over an 8 day period from December 22, 1993, to December 29, 1993, and again from January 1, 1994, to January 2, 1994. On December 20-21, 1993, a warm front of apparent Gulf Stream origin progresses northward through the array, crossing over several shelf mooring sites. By December 26-27, 1993, a large bolus of warm water shoreward of the Gulf Stream proper is impinging on mooring line D (the N-S oriented mooring line along the 60 m isobath). A narrow line of warm water exists shoreward of that bolus, running from about mooring A2 to B2 in box N, convex shoreward, and extending into box S to moorings C1 and C2. Four days later, on December 31, 1993, to January 1, 1994, warm Gulf Stream water is again seen impinging on the moorings situated at the 60 m isobath (A3, B3, C3, D1, and D2). This appears to be the remains of the large bolus of warm water apparent in the previous images but may be warm water originating from the next Gulf Stream meander that passes by. *Glenn and Ebbesmeyer* [1994b] found meanders progressing past Cape Hatteras with an ~4.6 day periodicity.

South of Cape Hatteras, *Glenn and Ebbesmeyer* [1994b] noted enhanced shoreward progression of Gulf Stream filament waters when the main Gulf Stream front is located farther from shore. In fact, during the period of along-shelf divergence shown in Figure 18 the Gulf Stream had moved offshore briefly, as indicated by the $B4_1$ pressure record (Figure 5). Pressure at mooring C4 also shows a more seaward Gulf

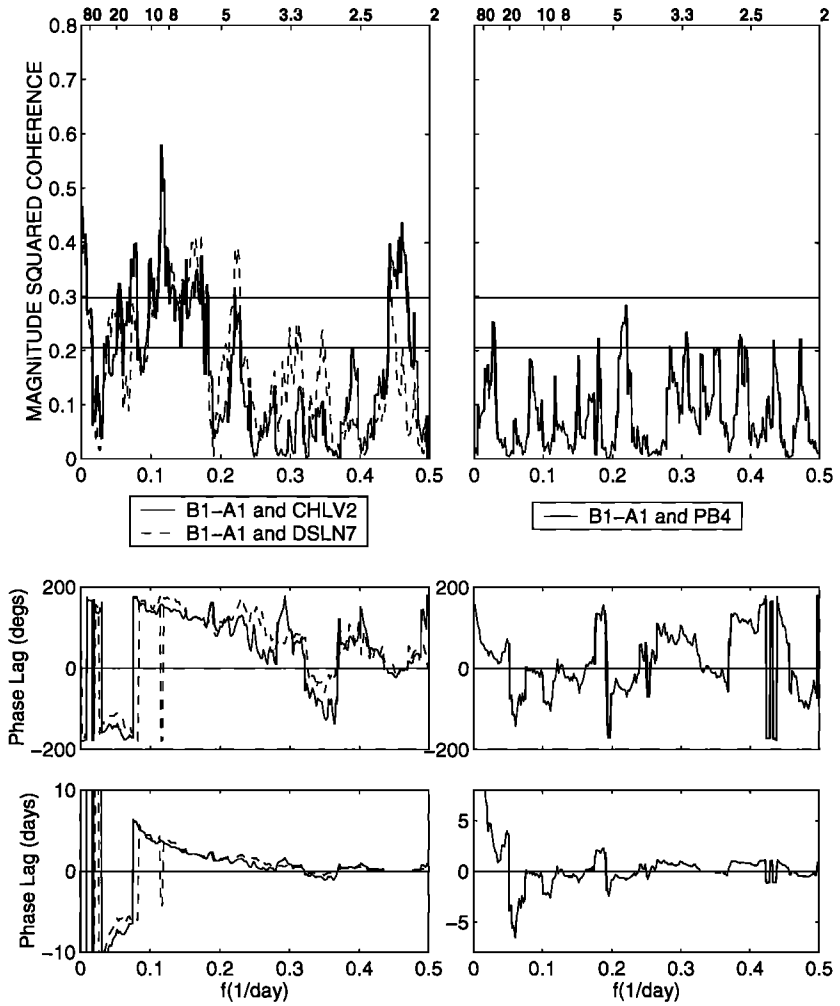

Figure 17. Cross spectra between nearshore transport convergence and forcing functions: (left) cross spectra between along-shelf transport convergence (B1-A1 transports) and CHLV2 along-shelf wind (solid line) and between along-shelf transport convergence and DSLN7 along-shelf wind (dashed line), (right) cross spectra between nearshore along-shelf transport convergence and P_{B4_1} (solid line), (top) magnitude squared coherence (drawn to the same scale), (middle) the phase lag in degrees, and (bottom) the phase lag in days, converted from degrees by $\theta_{day} = \theta_{deg}/(f360)$, where f is frequency. Positive phase lags indicate that the first quantity in the pair leads the second. Horizontal lines in the top panels show the 99% and 95% confidence levels.

Stream position (not shown). The C4 mooring location is coincident with mooring 3 of *Glenn and Ebbesmeyer* [1994b]. Their mooring helped to define the line along which they defined Gulf Stream distance from the shelf from AVHRR satellite SST imagery. There they saw extended periods (several months) during which the Gulf Stream was in either a "large" or "small" meander mode, as defined by the relative wavelengths and lateral amplitudes of the meanders associated with either mode and the Gulf Stream distance offshore at this location. The pressure records at B4 and C4 from the present study, on the other hand, indicate that during this study period the Gulf Stream occupied its most seaward location for only brief periods. However, the 30-90 day periodicity in the pressure records at B4 is also apparent in the $C4_1$ pressure data, and the records are coherent between the sites (not shown). This may be another manifestation of the same shifting between modes that *Glenn and Ebbesmeyer* [1994b] showed.

While along-shelf divergence occurred in box N only about 10% of the experiment time, along-shelf flow in box S was divergent 34% of that time. This rather large difference likely reflects differences in the character of the Gulf Stream's influence on off-shelf transport within the two regimes (i.e., immediately north and south of Cape Hatteras). South of the B mooring line along the seaward edge of box S, the mean position of the shoreward Gulf Stream edge follows the continental shelf break quite closely. The Gulf Stream provides a direct effect because of the meanders of the stream that propagate northeastward through this area [*Webster*, 1961; *Bane et al.*, 1981; *GlennEbbesmeyer*, 1994a,1994b]. These meanders dominate the cross-isobath flow at the shelf edge there. As first discussed by *Webster* [1961], there is a skew-

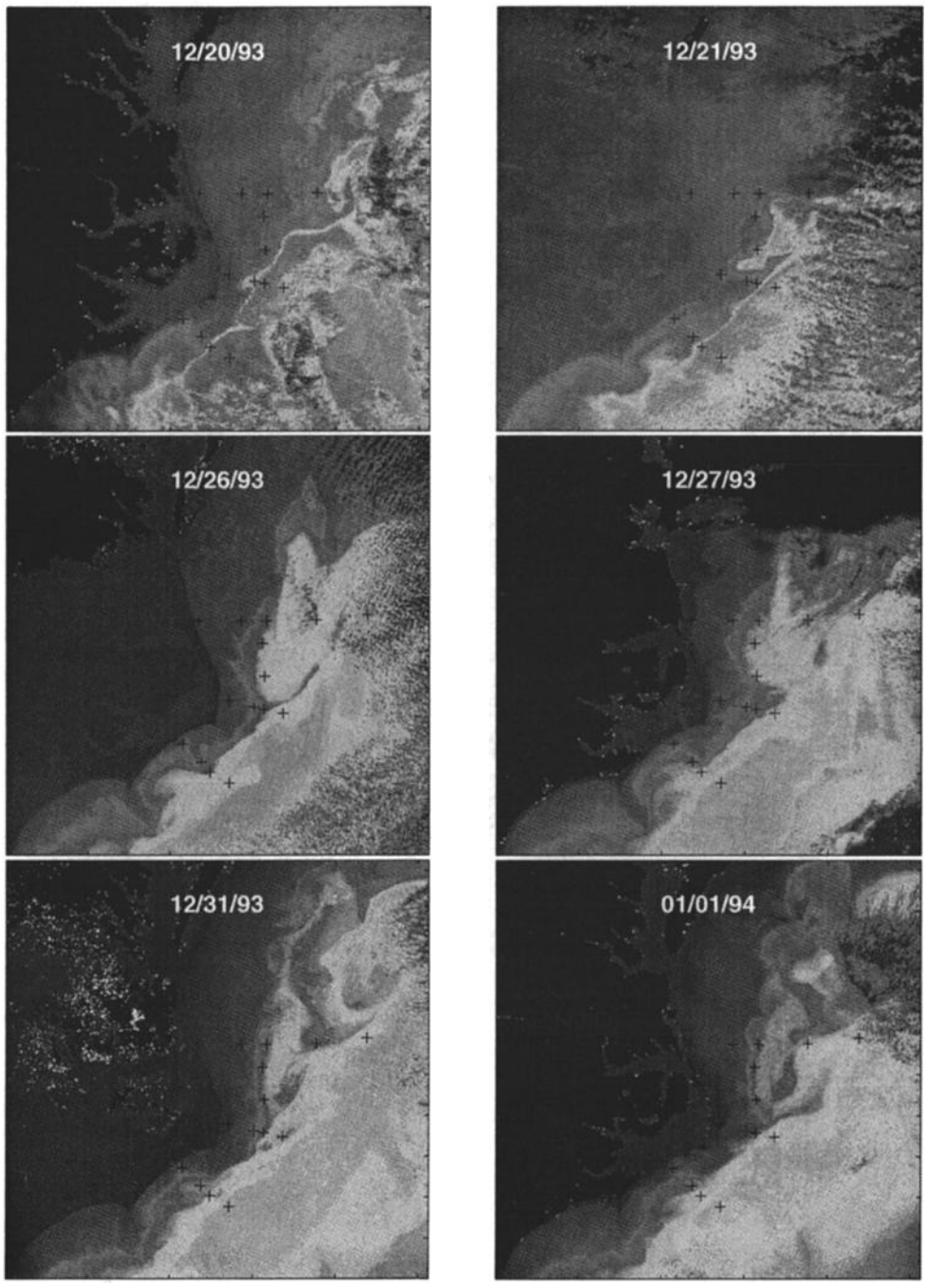

Figure 18. Sequence of AVHRR SST images during the December 1993 along-shelf divergence event in box N, north of Cape Hatteras.

ness in the meander pattern in this region that likely accounts for along-shelf convergence (and thus off-shelf export) approximately two thirds of the time. There is intense offshore flow associated with an approaching meander crest, and this segment of a meander is typically more elongated along stream than the less intense onshore flow segment of an approaching meander trough. ("Crest" refers to the shoreward-most portion of a meander; "trough" refers to the seaward-most portion.) North of line B, the Gulf Stream has separated from the shelf break, and the stream provides more of a remote forcing at the seaward edge of box N [*Bane et al.*, 1988]. The events that provide shoreward flow across the shelf break there [*Churchill and Cornillon*, 1991; *Churchill and Berger*, 1998] occur much less frequently than do the meanders that nearly continuously pass along the shelf edge south of Cape Hatteras.

Onshore flow over the shelf during periods of along-shelf divergence of sufficient magnitude to carry pollutants into the delicate ecosystems of coastal North Carolina or to consistently transport populations of larval fish shoreward clearly has not been proven nor disproven by this work. However, the clues gained here suggest that such transport is possi-

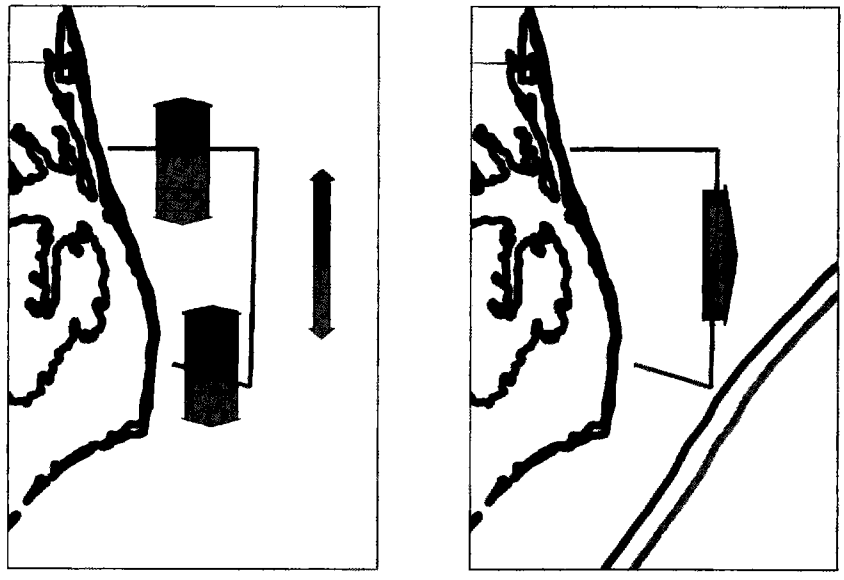

Figure 19. Schematic of the effects of along-shelf wind and Gulf Stream position on shelf transport near Cape Hatteras. (left) Along-shelf winds result in convergent along-shelf transport in the same direction as the wind. Solid arrows represent northward along-shelf wind and transport components; shaded arrows represent southward along-shelf wind and transport components. The shelf mooring lines A, B, and D, are shown as straight shaded lines. Winds are represented by the arrows to the right of the mooring box. Along-shelf transports are represented by arrows across the north and south boundaries of the box defined by the mooring lines. (right) The magnitude of the offshore transport implied by the along-shelf transport convergence is related to the Gulf Stream distance offshore, with more shoreward position associated with higher off-shelf export. The bold lines in the bottom right of the panel represent two possible offshore positions for the Gulf Stream edge; the arrows across the eastern face of box N represent offshore export across that face. The solid line and offshelf transport arrow represent a more shoreward Gulf Stream position; the shaded line and offshelf transport arrow represent a more seaward Gulf Stream position.

ble a significant fraction of the time. Further study of the conditions favorable for along-shelf divergence and of the resulting cross-shelf current structure needs to be pursued.

8. Discussion and Summary

Along-shelf transports across three cross-shelf lines on the continental shelf near Cape Hatteras have been calculated from moored current meter data over a period of 2 years. The along-shelf convergence has been calculated and used to infer cross-shelf transport, assuming continuity and no flow through the shoreward boundary. Transport and transport convergence have been related to wind and Gulf Stream forcing and to variability in sea level at the coast. Several interesting features of the flow have emerged from this study.

Along-shelf transport is predominantly convergent near Cape Hatteras, implying a mean offshore export in boxes N and S. The source of this mean convergence has not been explored, but is consistent with mean along-shelf pressure gradient forces in the South Atlantic Bight and Mid-Atlantic Bight directed toward Cape Hatteras. Such pressure gradients have been considered in the past by numerous authors [e.g., *Stommel and Leetmaa*, 1972; *Sturges*, 1974; *Bush and Kupferman*, 1980; *Csanady*, 1979; *Lee et al.*, 1985]. The along-shelf transport variability is primarily wind-driven and is highly correlated with sea level fluctuations at the coast. Poleward (equatorward) winds are associated with poleward (equatorward) transport and set-down (set-up) at the coast. Winds lead the transport by half a day or less and lead the sea level by a similar amount. Transport leads sea level by a few hours at long periods, but no clear lead-lag relationship is apparent at periods shorter than 8 days. Annual variability is apparent in winds and transports. Transport is not well correlated with Gulf Stream offshore position. Both the cross spectral analysis and the EOF analysis illustrate that fluctuations in along-shelf transport are closely tied to wind field variability across a wide frequency band (2-20 days) despite high energy variability in the Gulf Stream at similar periods. A schematic is shown illustrating the sense of the relationship between along-shelf wind direction and shelf transport across mooring lines A and B (Figure 19).

The along-shelf convergence variability is highly correlated with Gulf Stream position offshore, with more shoreward Gulf Stream position leading increased along-shelf convergence by hours to a few days (see the summary schematic in Figure 19). Long-period variability of 14-16 month period is apparent in both Gulf Stream position and transport convergence. In addition, a 1-3 month period variability is identified in both along-shelf transport convergence and Gulf Stream offshore position. There is also high coherence between Gulf Stream position and transport convergence at the 4-6 day and 9-10 day period bands. Neither Gulf Stream

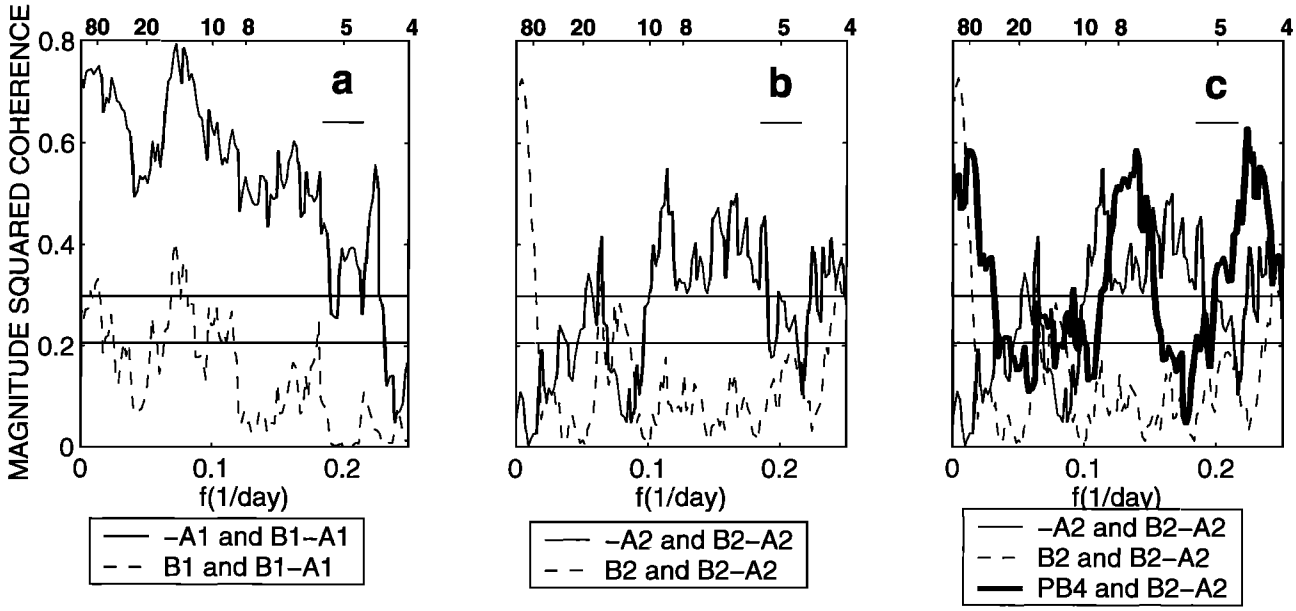

Figure 20. Cross spectra between transports and transport convergence. (a) Magnitude squared coherence between nearshore along-shelf transports and nearshore along-shelf convergence (B1-A1 transports): A1 with convergence (solid line) and B1 with convergence (dashed line). (b) Magnitude squared coherence between midshelf along-shelf transports and midshelf convergence (B2-A2 transports): A2 with convergence (solid line) and B2 with convergence (dashed line). (c) Same as (b), with the addition of the magnitude squared coherence between the Gulf Stream proxy and midshelf transport convergence, as in Figure 11 (bold solid line). Horizontal lines show the 99% and 95% confidence levels.

position nor along-shelf transport convergence is coherent with coastal sea level variability at long periods. Variability in along-shelf convergence, on the other hand, is poorly correlated with wind or wind convergence variability.

It is somewhat puzzling that the difference between transports across mooring lines A and B, both highly correlated with the along-shelf wind over a broad frequency band, should itself show such poor coherence with the wind. A comparison with the nearshore case is instructive. At the 20 m isobath, along-shelf convergence (B1-A1) is poorly correlated with the Gulf Stream proxy, as discussed in section 6. Coherence with the wind is somewhat better but still weak over essentially all frequency bands (Figure 17). However, the nearshore convergence shows strong coherence with transport at mooring A1 across a broad band of frequencies but poor coherence with transport at B1 (Figure 20). Suppose that the transports at A1 and B1 are each composed of two parts, some part that is well correlated between lines A and B and of equivalent magnitude between them (presumed but not required to be predominantly wind-forced, subscript w), and some other excess part that is not coherent between the two mooring lines (subscript o): $A1 = A1_w + A1_o$, and $B1 = B1_w + B1_o$, with $A1_w = B1_w$. This should be especially true in the frequency bands where transports and winds are most coherent. Then the convergence in a given frequency band is $Cnv1 = B1_w + B1_o - A1_w - A1_o = B1_o - A1_o$. The coherence between transport across either line and convergence at a given frequency should then be a measure of the contribution of this excess (presumably non-wind-driven) part of the transport. Stated another way, if everything added to the box at a given frequency at one end is subtracted at the other end, no convergence at that frequency should result, and no coherence between transport and transport convergence would exist at that frequency. What coherence does exist must be due to the part entering the box at one end with no matching component at the other. In the nearshore case currently under discussion the convergence is highly coherent with A1 transport over a broad band of frequencies but poorly coherent with B1 transport. Most of what enters or leaves the box at B1 is matched by an equivalent component at A1. On the contrary, some part of what enters or leaves the box at A1 is not matched by an equivalent component at B1. That is, $B1_o$ appears to be an insignificant contributor to Cnv1, while much of the Cnv1 signal can be accounted for by $A1_o$. Neither the wind nor the Gulf Stream appear to be the source of that variability, given the low coherence of A1 or B1-A1 with either (Figure 17).

On the midshelf the convergence ($Cnv2 = B2 - A2$) is coherent with both B2 and A2 over limited frequency bands (Figure 20) but at generally lower levels than are seen between Cnv1 and A1 in the nearshore case. Therefore midshelf convergence cannot be easily accounted for solely by excess transport across lines A or B ($A2_o$ or $B2_o$), especially in frequency bands where coherence with both B2 and A2 is low. Additionally, in some of those bands where neither transport component can account for the convergence, high correlation is seen with the Gulf Stream position offshore (Figures 11 and 20). Herein it is hypothesized that export processes across line D are affected by the Gulf Stream

proximity, such that through continuity that component of the convergence appears in $Cnv2 = B2_o - A2_o$. This is consistent with P_{B4_1} fluctuations leading transport convergence fluctuations, as seen in the cross spectral analyses. Nearshore, convergence can be accounted for by excess flow across mooring line A. On the midshelf neither excess flow across line A nor across line B can adequately account for the convergence seen there, and processes affecting flow across line D must also be considered.

Despite predominantly convergent flow on the shelf at Cape Hatteras, brief periods of along-shelf divergence and shoreward cross-shelf transport do exist. This happens ~10% of the time in box N, during episodes of 1-8 days duration. South of Cape Hatteras, divergence is more common, occuring approximately a third of the time in box S. This difference may signify a change in the nature of stream-shelf flow interaction between the two regimes north and south of Cape Hatteras. The divergence events in box N occur preferentially during northward transport events on the shelf, when the Gulf Stream location is seaward of its mean location. The implied and tentatively identified onshore flows of a few cm s^{-1} are not necessarily of sufficient magnitude to carry shelf edge parcels of water across the narrow shelf to the coast over such short periods. However, satellite imagery for an extended along-shelf divergent period clearly suggests that shelf edge parcels could be advected a significant fraction of the way across the shelf. This process deserves more study.

Previous authors have described mechanisms of shelf water export near Cape Hatteras that clearly implicate the Gulf Stream or Gulf Stream filaments [*Lillibridge et al.*, 1990; *Churchill and Cornillon*, 1991; *Churchill and Berger*, 1998]. In this paper, the clear correlation between Gulf Stream variability and along-shelf transport convergence, and therefore with off-shelf export over an extended period of time encompassing all seasons, is highlighted for the first time. Presumably, the Gulf Stream variability alters the effectiveness of various export mechanisms through filament-shelf water interaction, through modulation of the cross-shelf sea level slope and through the magnitude and extent of Gulf Stream intrusions onto the shelf.

Acknowledgments. This work was supported through ONR grant N00014-97-1-0500. The data were collected for the Minerals Management Service OCS Study MMS 94-0047 under MMS Contract 14-35-0001-30599. Brian Blanton acquired the wind and sea level data from the collection agencies and processed them to the form in which they are used here. Final draft preparation was done using computer resources at NOAA/PMEL, Seattle, Washington, and at the Center for Coastal Physical Oceanography, Old Dominion University, Norfolk, Virginia.

References

Bane, J. M., D. A. Brooks, and K. R. Lorenson, Synoptic observations of the three-dimensional structure and propagation of Gulf Stream meanders along the Carolina continental margin, *J. Geophys. Res.*, *86*, 6411–6425, 1981.

Bane, J. M., O. B. Brown, R. H. Evans, and P. Hamilton, Remote forcing of shelfbreak currents by the Gulf Stream in the Mid-Atlantic Bight, *Geophys. Res. Lett.*, *15*, 405–407, 1988.

Berger, T. J., P. Hamilton, R. J. Wayland, J. O. Blanton, W. C. Boicourt, J. H. Churchill, and D. R. Watts, A physical oceanographic field program offshore North Carolina, *Tech. Rep. OCS Study MMS 94-0047*, U.S. Dep. of the Inter., Miner. Manage. Serv., New Orleans, La., 1995.

Biscaye, P. E., C. N. Flagg, and P. G. Falkowski, The Shelf Edge Exchange Processes Experiment, SEEP-II: An introduction to hypotheses, results and conclusions, *Deep Sea Res., Part II*, *41*, 231–252, 1994.

Blanton, B. O., Transport near Cape Hatteras: A model-based study, Master's thesis, 135 pp., Univ. of N.C., Chapel Hill, 2001.

Blanton, J. O., F. B. Schwing, A. H. Weber, L. J. Pietrafesa, and D. W. Hayes, Wind stress climatology in the South Atlantic Bight, in *Oceanography of the Southeastern U.S. Continental Shelf, Coastal Estuarine Sci., vol. 2*, edited by L. P. Atkinson, D. W. Menzel, and K. A. Bush, pp. pp. 23–32, AGU, Washington, D.C., 1985.

Brooks, D. A., and J. M. Bane, Gulf Stream fluctuations and meanders over the Onslow Bay upper continental shelf, *J. Phys. Oceanogr.*, *11*, 247–256, 1981.

Brooks, D. A., and J. M. Bane, Gulf Stream meanders off North Carolina during winter and summer, 1979, *J. Geophys. Res.*, *88*, 4633–4650, 1983.

Bush, K., and S. L. Kupferman, Wind stress direction and alongshore pressure gradient in the Middle Atlantic Bight, *J. Phys. Oceanogr.*, *10*, 469–471, 1980.

Checkley, D. M., S. Raman, G. L. Maillet, and K. M. Mason, Winter storm effects on the spawning and larval drift of a pelagic fish, *Nature*, *335*, 346–348, 1988.

Churchill, J. H., and T. J. Berger, Transport of Middle Atlantic Bight shelf water to the Gulf Stream near Cape Hatteras, *J. Geophys. Res.*, *103*, 30,605–30,622, 1998.

Churchill, J. H., and P. C. Cornillon, Gulf Stream water on the shelf and upper slope north of Cape Hatteras, *Cont. Shelf Res.*, *11*, 409–431, 1991.

Csanady, G. T., The pressure field along the western margin of the North Atlantic, *J. Geophys. Res.*, *84*, 4905–4915, 1979.

Csanady, G. T., *Circulation in the Coastal Ocean*, 279 pp., D. Reidel, Norwell, Mass., 1982.

Gawarkiewicz, G., T. G. Ferdelman, T. M. Church, and G. W. Luther, Shelfbreak frontal structure on the continental shelf north of Cape Hatteras, *Cont. Shelf Res.*, *16*, 1751–1773, 1996.

Glenn, S. M., and C. C. Ebbesmeyer, The structure and propagation of a Gulf Stream frontal eddy along the North Carolina shelf break, *J. Geophys. Res.*, *99*, 5029–5046, 1994a.

Glenn, S. M., and C. C. Ebbesmeyer, Observations of Gulf Stream frontal eddies in the vicinity of Cape Hatteras, *J. Geophys. Res.*, *99*, 5047–5055, 1994b.

Hare, J. A., and R. K. Cowen, Expatriation of *Xyrichtys novacula* (pisces: Labridae) larvae: Evidence of rapid cross-slope exchange, *J. Mar. Res.*, *49*, 801–823, 1991.

Hare, J. A., and R. K. Cowen, Transport mechanisms of larval and pelagic juvenile bluefish *pomatomus saltatrix* from South Atlantic Bight to Mid-Atlantic Bight nursery habitats, *Limnol. Oceanogr.*, *41*, 1264–1280, 1996.

Hogg, N. G., Mooring motion corrections revisited, *J. Atmos. Oceanic Technol.*, *8*, 289–295, 1991.

Johns, W., and D. R. Watts, Time scales and structure of topographic Rossby waves and meanders in the deep Gulf Stream, *J. Mar. Res.*, *44*, 267–290, 1986.

Lee, T. N., V. Kourafalou, J. D. Wang, W. J. Wo, J. O. Blanton, L. P. Pietrafesa, L. P. Atkinson, and L. J. Pietrafesa, Shelf circulation from Cape Canaveral to Cape Fear during Winter, in *Oceanography of the Southeastern U.S. Continental Shelf, Coastal Estuarine Sci., vol. 2*, edited by L. P. Atkinson, D. W. Menzel, and K. A. Bush, pp. pp. 33–62, AGU, Washington, D.C., 1985.

Lee, T. N., J. A. Yoder, and L. P. Atkinson, Gulf Stream frontal eddy influence on productivity of the southeast U.S. continental shelf, *J. Geophys. Res.*, *96*, 22,191–22,205, 1991.

Lillibridge, J. L., G. Hitchcock, T. Rossby, E. Lessard, M. Mork, and L. Golmen, Entrainment and mixing of shelf/slope waters in the near-surface Gulf Stream, *J. Geophys. Res.*, *95*, 13,065–13,087, 1990.

Linder, C. A., and G. Gawarkiewicz, A climatology of the shelf-break front in the Middle Atlantic Bight, *J. Geophys. Res.*, *103*, 18,405–18,423, 1998.

Manning, J., Middle Atlantic Bight salinity: Interannual variability, *Cont. Shelf Res.*, *11*, 123–137, 1991.

Percival, D. B., and A. T. Walden, *Spectral Analysis for Physical Applications: Multitaper and Conventional Univariate Techniques*, 583 pp., Cambridge Univ. Press, New York, 1993.

Pickart, R. S., and W. M. Smethie, How does the Deep Western Boundary Current cross the Gulf Stream?, *J. Phys. Oceanogr.*, *24*, 2602–2616, 1994.

Quinlan, J. A., B. Blanton, T. Miller, and F. Werner, From spawning grounds to the estuary: using linked individual based and hydrodynamic models to interpret patterns and processes in the oceanic phase of Atlantic menhaden brevoortia tyrannus life history, *Fish. Oceanogr.*, *8, suppl. 2*, 224–246, 1999.

Stegmann, P. M., and J. A. Yoder, Variability of sea-surface temperature in the South Atlantic Bight as observed from satellite: Implications for offshore spawning fish, *Cont. Shelf Res.*, *16*, 843–861, 1996.

Stommel, H., and A. Leetmaa, Circulation on the continental shelf, *Proc. Natl. Acad. Sci. U.S.A.*, *69*, 3380–3384, 1972.

Sturges, W., Sea level slope along continental boundaries, *J. Geophys. Res.*, *79*, 825–830, 1974.

Walsh, J. J., P. E. Biscaye, and G. T. Csanady, The 1983-1984 Shelf Edge Exchange Processes Experiment (SEEP-I) experiment: Hypotheses and highlights, *Cont. Shelf Res.*, *8*, 435–456, 1988.

Webster, F. A., A description of Gulf Stream meanders off Onslow Bay, *Deep Sea Res.*, *8*, 130–143, 1961.

Werner, F., B. Blanton, J. A. Quinlan, and R. Luettich, Physical oceanography of the North Carolina continental shelf during the fall and winter seasons: Implications for the transport of larval menhaden, *Fish. Oceanogr.*, *8, suppl. 2*, 7–21, 1999.

Dana K. Savidge, Center for Coastal Physical Oceanography, Department of Ocean, Earth and Atmospheric Sciences, Old Dominion University, Norfolk, VA 23529. (savidge@ccpo.odu.edu)

John M. Bane Jr., Department of Marine Sciences, University of North Carolina at Chapel Hill, CB 3300, 12-7 Venable Hall, Chapel Hill, NC 27599. (bane@unc.edu)

(Received July, 27, 2000; revised February, 26, 2001; accepted March, 7, 2001.)